

Final Report on the Fixed-Point Comparison of Au/Pt thermocouples

## APMP.T-S4

Prepared by

Yong-Gyoo Kim<sup>1)</sup>, Hans Liedberg<sup>2)</sup> and Ferdouse Jahan<sup>3)</sup>

<sup>1)</sup> Korea Research Institute of Standards and Science (KRISS), Korea

<sup>2)</sup> National Measurement Institute of South Africa (NMISA), South Africa

<sup>3)</sup> National Measurement Institute of Australia (NMIA), Australia

February 5, 2008

## Table of Contents

1. Introduction	3
2. Summary of Comparison	3
3. Measurement Schedule	4
4. Preparation of the thermocouples	4
5. Measurements Results by the Participants	6
6. Final Measurements by the Pilot Lab	15
7. Uncertainty Evaluation	19
8. Comparison Data Analysis	20
9. References	28
Appendix A. Protocol	29
Appendix B. Description of the measuring devices of participants	36
Appendix C. Uncertainty evaluation tables	39

## 1. Introduction

The Au/Pt thermocouple is the most accurate thermocouple below the Ag fixed-point temperature and is widely used in many NMIs (National Measurement Institutes) to disseminate the ITS-90 temperature scale in their countries.

In 2002, at the Temperature Symposium in Chicago, USA, the need for the international comparison for the Au/Pt thermocouple was raised during an informal communication by some participants and three NMIs (KRISS, NMIA, NMISA) were agreed to conduct the comparison. The objective of this comparison is to assess the degree of equivalence of the calibration results at the fixed-points. The fixed-points chosen were Ga, Sn, Zn, Al and Ag. The names of the participating laboratories and the contact persons are given in Appendix A.

KRISS was invited to be the pilot laboratory of this comparison and asked to prepare the circulating artifacts. The protocol of this comparison was circulated on April 2003 by the pilot lab. After calibration by the pilot labs, thermocouples were sent out to one of the participating laboratories. After the measurements at the first lab, they were moved to the next lab. Finally thermocouples were sent back to the pilot lab and measured once again to check the stability of the artifacts.

This report includes the raw measurement data and their associated uncertainties as given by the participants, the equipments used in the comparisons.

## 2. Summary of Comparison

Round robin comparison was used because of the small number of the participants. The pilot laboratory, KRISS (Korea) prepared two Au/Pt thermocouples (serial numbers: BC-0301 and BC-0302). The thermocouples were designed so that their thermal emfs were to be compared at the Ga, Sn, Zn, Al and Ag fixed-points.

The thermocouples were transferred to NMISA (Rep. South Africa) by air flight. NMISA sent the artifacts to NMIA (Australia) after calibration. Finally KRISS received the thermocouples and recalibrated them.

The comparison protocol is given in Appendix A. All the equipments used in the comparison are listed in Appendix B. In Appendix C, uncertainty budget tables are given at each fixed-point.

## 3. Measurement Schedule

The measurement schedule was set in the protocol, but due to several reasons the schedule was changed. The actual comparison schedule is summarized below.

- January ~ April 2003 : Design and calibration of the artifacts by the pilot lab (KRISS)
- May 2003 : Transferred to NMISA
- June 2003 : Transferred to NMIA
- February 2004 : thermocouples repaired in NMIA
- April 2005 : Sent back to KRISS and recalibrated
- May 2005 ~ November 2006 : Special tests were performed at the Ag point by KRISS because thermal emfs at silver point were found to be dependent on the furnaces used for the realization of freezing temperature.
- August 2007: Draft report prepared by the pilot lab.
- September 2007: Draft A circulated to the participating labs.
- December 2007: Draft B circulated to the participating labs.

#### 4. Preparation of the thermocouples

##### 4.1 Wires

Au and Pt wires were from the Heraeus Company. Their nominal purity was 99.999 % for Au, 99.9999 % for Pt. In Table 1, chemical impurities from manufacturer are presented.

##### 4.2 Annealing of wires and alumina insulators

Pt wires were electrically annealed at about 1300 °C for 30 min. The wire temperature was lowered to about 450 °C, then annealed overnight. 70 cm of Au wires were annealed at 1000 °C for 5 h followed by furnace cooling. Two wires were welded together after annealing.

Twin-bore alumina insulators were from McDanel (AXD-1008). It was 60 cm long and 3.18 mm in diameter. The bore size was 1.02 mm. These insulators were pre-baked at 1500 °C for 1 h before use.

Table 1. Impurity analysis of the test wires

Au		Pt	
Elements	Content /ppm	Elements	Content /ppb
Ag	1.6	Au	130
Cu	<1.0	Ag	<20
Si	<1.0	Pd	145
Fe	<2.0	Ir	88
Mg	<1.0	Rh	255
Pb	<1.0	Other	<350

##### 4.3 Preparation of measuring junction

Thin Au wire of 0.1 mm diameter was used to make a hot junction. The junction was a bridge-type where a thin wire connected the thermoelements.

#### 4.4 Assembly of test thermocouples

After inserting the thermocouple wires into the alumina insulator, they were assembled with polyvinyl insulator. The thermocouples were inserted into the quartz protecting tubes with an inner diameter of 5 mm and length of 59 cm. The ice junction section was inserted into the 3/8" stainless steel tube with length of about 20 cm. The quartz tube was sand-blasted to protect from the light-piping effect. The test thermocouples were designated as BC-0301 and BC-0302.

#### 4.5 Final furnace annealing

Two thermocouples were annealed at 1000 °C in the vertical annealing furnace (ATF-V-01) at an immersion depth of 46 cm from the furnace opening. Au/Pt thermocouples were annealed for 10 h, and then removed from the furnace quickly to be cooled rapidly. In Fig.1, the temperature profile measured at the set temperature of 1000 °C was presented. The measuring thermometer was a Pt/Pd thermocouple. Most of the temperature gradient was formed in range of 10 cm from the furnace opening.

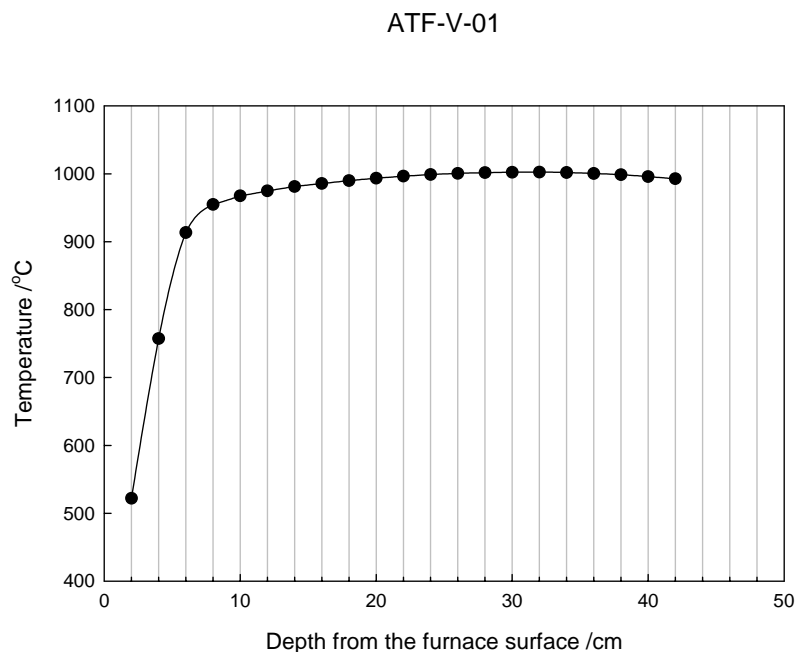


Fig.1. Temperature gradient profile for ATF-V-01 furnace

Note : The thermocouples were uniformly annealed 360 mm from the tip.

## 5. Measurement Results by the Participants

### 5.1. Measured emf values

Table 2 summarizes the measurement results by the KRISS before the circulation. The fixed-point emf values and their standard deviations are listed. The melting/freezing plateau stability is also shown in terms of the standard deviation.

Table 3 and 4 show the measurement results by the NMISA and NMIA, respectively. From the NMISA some comments were reported as following.

*“Note: The wire of BC-0301 may have been stressed near the top of the reference junction during measurements at NMISA, causing the emf to drop as the level of the ice point drops slightly. (Compare the relatively constant emf at Al with the dropping emf at Zn and Sn. The temperature near the bottom of the ice point was checked using an IPRT: it remained stable to within 1 mK during one hour in the fluidised bath enclosure.) It is hoped that the first measurements of BC-0301 more closely represent unstressed wire. For this reason, the mean values listed above are seldom of the last 10 minutes of measurements.”*

At the NMISA, the measurement data have been corrected for DVM drift, assuming a constant drift rate between the 18 February and 23 June 2003 calibrations. The uncertainty ( $k = 1.732$ ) was manufacturer’s 1-year specification for ppm of reading + measured drift over 4 months / 4.

At the NMIA, during the measurement, both thermocouples were open-circuited. The gold wire was disconnected from the platinum leg. These two thermocouples were repaired under the instruction of the pilot laboratory. Finally all measurements were completed.

Figures 2 to 4 show the typical melting/freezing plateaus for BC-0301 thermocouple by the participants at each fixed-point.

Table 2. Measurement results by KRISS before circulation

Thermocouple	Emfs at fixed-points / $\mu\text{V}$				
	Ga	Sn	Zn	Al	Ag
BC-0301 ( $\pm 1 \sigma$ )	$196.32 \pm 0.03$	$2235.74 \pm 0.04$	$4944.69 \pm 0.03$	$9318.67 \pm 0.03$	$16119.49 \pm 0.04$
	$196.36 \pm 0.02$	$2235.66 \pm 0.04$	$4944.62 \pm 0.04$	$9318.71 \pm 0.02$	$16120.30 \pm 0.04$
	$196.35 \pm 0.02$	$2235.73 \pm 0.04$	$4944.63 \pm 0.02$	$9318.72 \pm 0.01$	$16119.69 \pm 0.03$
	$196.34 \pm 0.02$	$2235.71 \pm 0.04$	$4944.65 \pm 0.04$	$9318.70 \pm 0.03$	$16119.83 \pm 0.42$
BC-0302 ( $\pm 1 \sigma$ )	$196.38 \pm 0.03$	$2235.77 \pm 0.03$	$4944.63 \pm 0.07$	$9318.83 \pm 0.02$	$16119.26 \pm 0.03$
	$196.36 \pm 0.02$	$2235.76 \pm 0.03$	$4944.74 \pm 0.03$	$9318.91 \pm 0.01$	$16119.34 \pm 0.03$
	$196.43 \pm 0.02$	$2235.80 \pm 0.03$	$4944.64 \pm 0.03$	$9318.88 \pm 0.01$	$16118.69 \pm 0.02$
	$196.39 \pm 0.03$	$2235.78 \pm 0.02$	$4944.67 \pm 0.06$	$9318.87 \pm 0.04$	$16119.10 \pm 0.35$

Table 3. Measurement results by NMISA

Thermocouple	Emfs at fixed-points / $\mu\text{V}$				
	Ga	Sn	Zn	Al	Ag
BC-0301 ( $\pm 1 \sigma$ )	$195.90 \pm 0.01$	$2235.34 \pm 0.01$	$4944.37 \pm 0.01$	$9318.54 \pm 0.01$	$16117.90 \pm 0.02$
	$195.92 \pm 0.01$	$2235.35 \pm 0.01$	$4944.32 \pm 0.01$	$9318.62 \pm 0.01$	$16117.89 \pm 0.02$
	$195.89 \pm 0.01$	$2235.34 \pm 0.01$	$4944.35 \pm 0.01$	$9318.63 \pm 0.01$	$16117.90 \pm 0.02$
	$195.90 \pm 0.02$	$2235.34 \pm 0.01$	$4944.35 \pm 0.02$	$9318.60 \pm 0.05$	$16117.90 \pm 0.01$
BC-0302 ( $\pm 1 \sigma$ )	$196.19 \pm 0.01$	$2235.62 \pm 0.02$	$4944.62 \pm 0.01$	$9318.86 \pm 0.01$	$16118.19 \pm 0.01$
	$196.17 \pm 0.01$	$2235.60 \pm 0.01$	$4944.60 \pm 0.01$	$9318.87 \pm 0.01$	$16118.16 \pm 0.01$
	$196.20 \pm 0.01$	$2235.62 \pm 0.01$	$4944.62 \pm 0.01$	$9318.93 \pm 0.01$	$16118.09 \pm 0.04$
	$196.19 \pm 0.01$	$2235.61 \pm 0.01$	$4944.61 \pm 0.01$	$9318.89 \pm 0.04$	$16118.15 \pm 0.05$

Table 4. Measurement results by NMIA

Thermocouple	Emfs at fixed-points / $\mu\text{V}$				
	Ga	Sn	Zn	Al	Ag
BC-0301	196.03	2235.36	4944.32	9318.34	16117.43
	196.01	2235.42	4944.28	9318.33	16117.36
	196.01	2235.37	4944.33	9318.31	16117.32
					16117.34
	$196.02 \pm 0.01$	$2235.38 \pm 0.03$	$4944.31 \pm 0.03$	$9318.33 \pm 0.02$	$16117.36 \pm 0.05$
BC-0302	196.11	2235.46	4944.41	9318.74	16117.46
	196.09	2235.45	4944.38	9318.70	16117.22
	196.11	2235.46	4944.39	9318.62	16117.40
					16117.27
	$196.10 \pm 0.01$	$2235.46 \pm 0.01$	$4944.39 \pm 0.02$	$9318.69 \pm 0.06$	$16117.34 \pm 0.11$

# BC\_0301\_KRISS

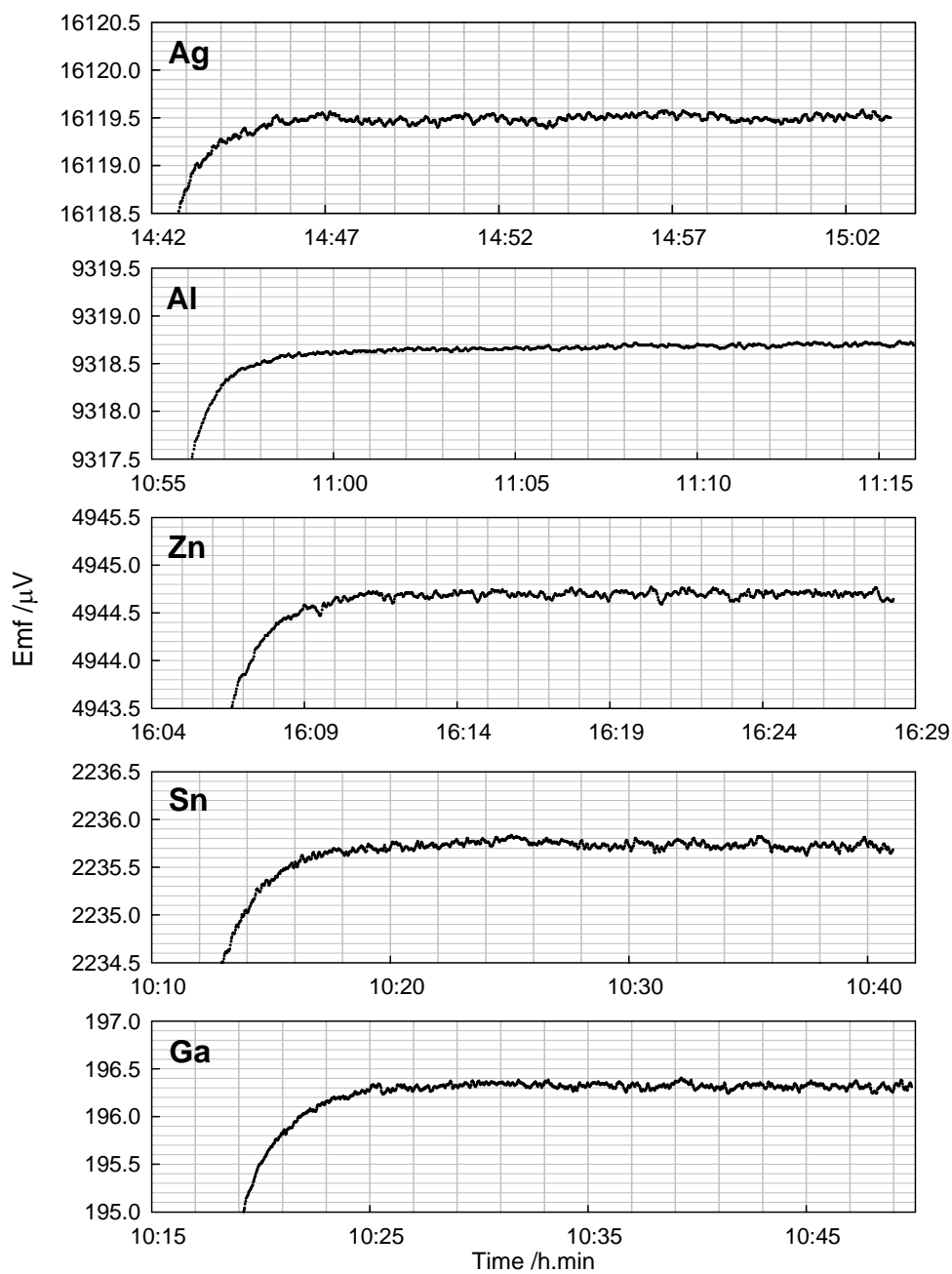


Fig. 2. Typical melting/freezing curves of BC-0301 at KRISS at each fixed-point.

BC\_0301\_NMISA

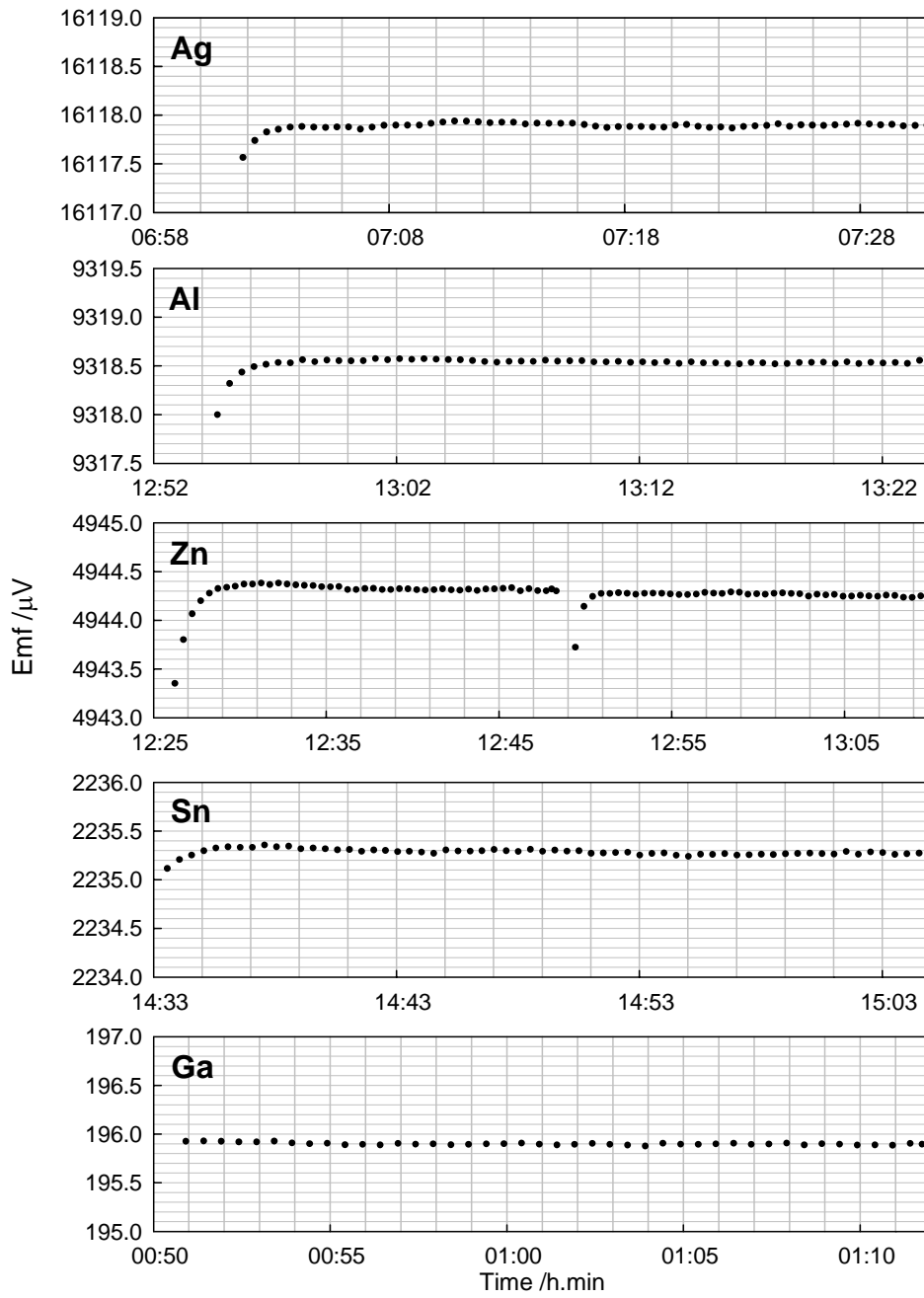


Fig. 3. Typical melting/freezing curves of BC-0301 at NMISA at each fixed-point.

# BC\_0301\_NMIA

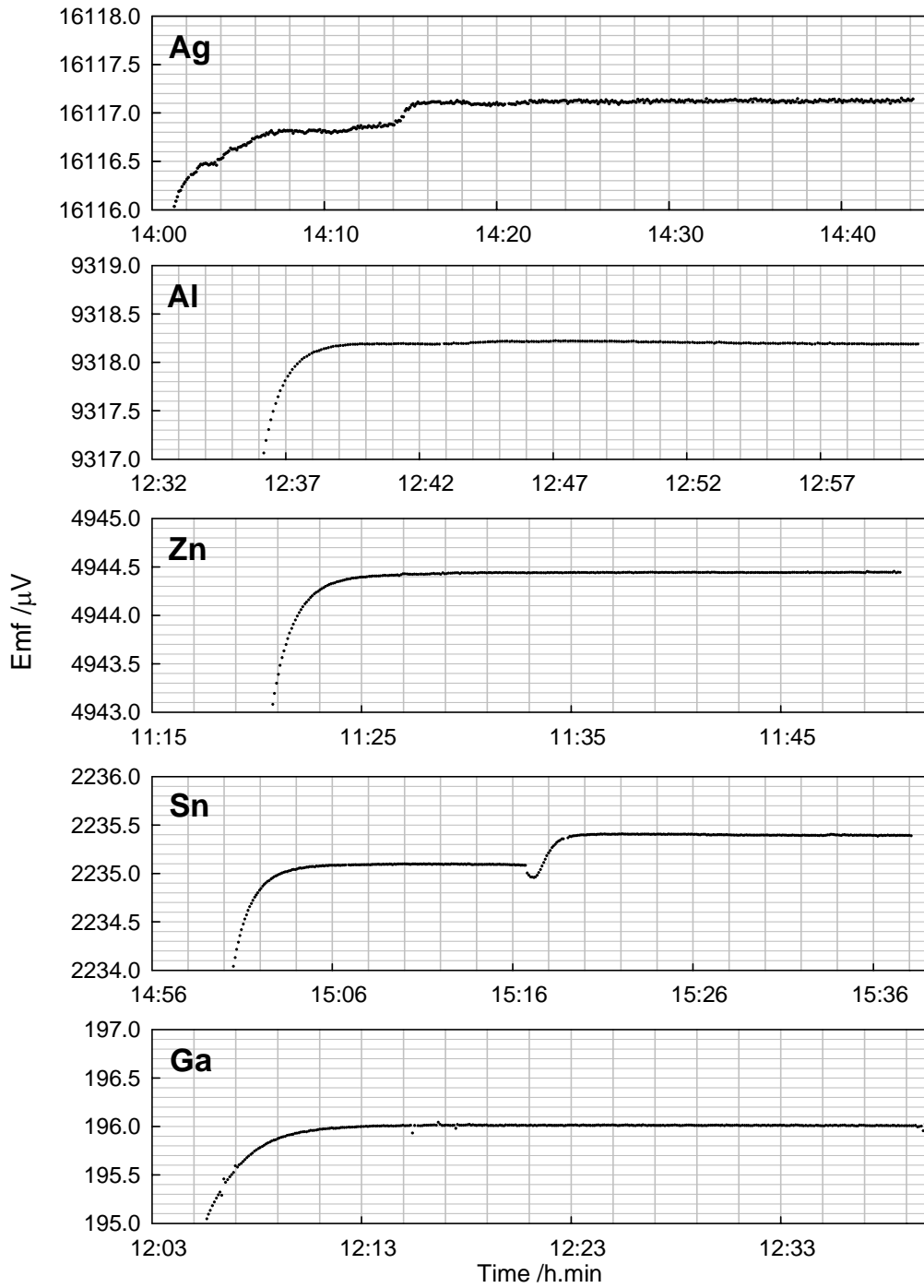


Fig. 4. Typical melting/freezing curves of BC-0301 at NMIA at each fixed-point.

## 5.2 Inhomogeneity test results

Figs.5 ~ 7 show the immersion profiles of thermocouples in the liquid bath. Test conditions are well described in appendix. For BC-0301, the maximum emf variation was within  $\pm 0.1 \mu\text{V}$ . In case of BC-0302, the variation was within  $\pm 0.1 \mu\text{V}$  at KRISS and NMIA, but at NMISA it was  $\pm 0.2 \mu\text{V}$ .

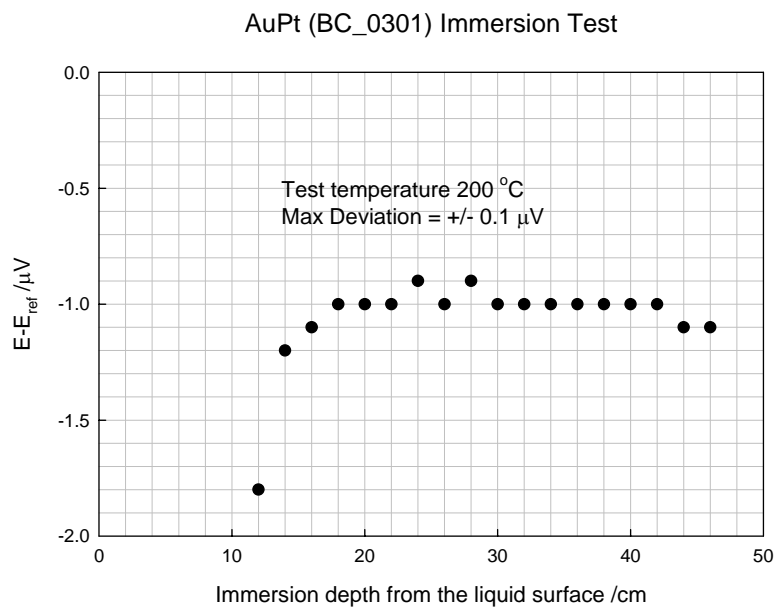


Fig.5 (a) Immersion result of BC-0301 by KRISS

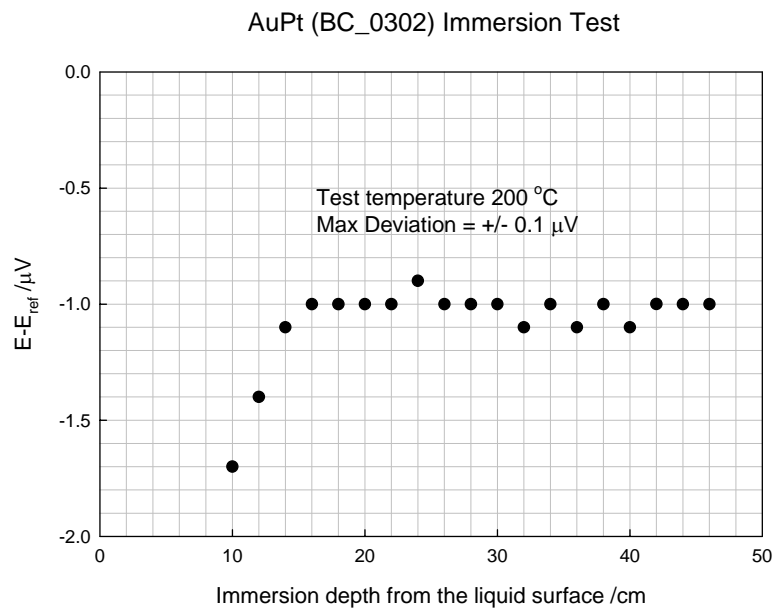


Fig.5 (b) Immersion result of BC-0302 by the KRISS

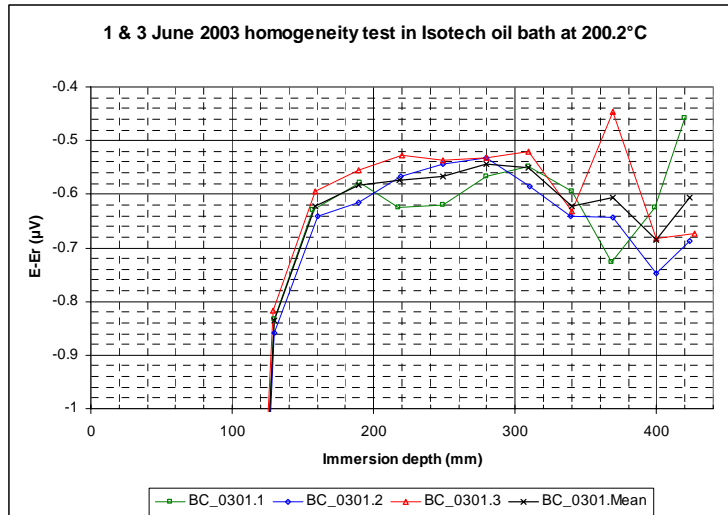


Fig.6(a) Immersion result of BC-0301 by the NMISA

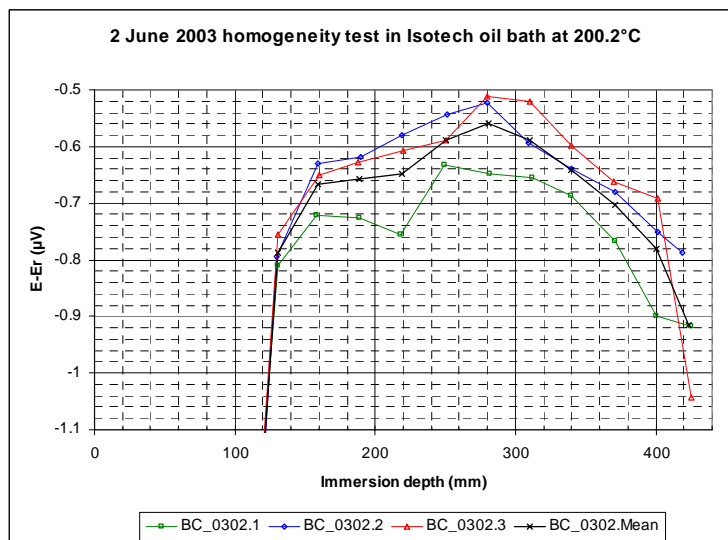


Fig.6(b) Immersion result of BC-0302 by the NMISA

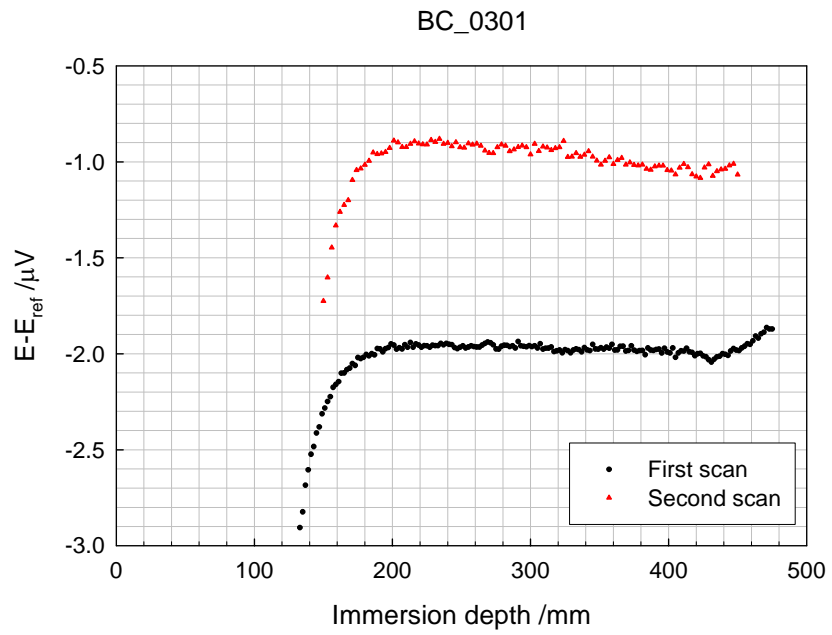


Fig.7(a) Immersion result of BC-0301 by the NMIA

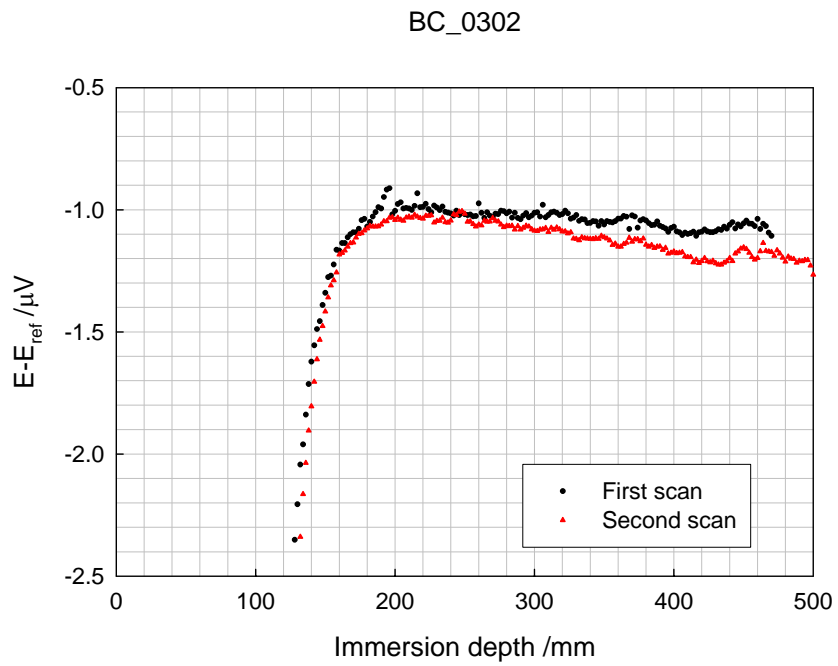


Fig.7(b) Immersion result of BC-0302 by the NMIA

### 5.3 Immersion tests of the IP section in the ice point by NMIA

During measurements of lower temperature fixed point it was observed that the measured EMF at the fixed point varies with the change of immersion length of the reference junction in the ice point. The effect of immersion of the reference junction was then assessed while realising Sn point. Fig. 8 shows the variation of measured EMF with the immersion length of the IP section in the ice point. For thermocouple BC-0301, EMF changed by  $0.3 \mu\text{V}$  when immersion changes by 3 cm, whereas for thermocouple BC-0302, the change was about  $0.1 \mu\text{V}$ . This is due to the inhomogeneity of IP section of the wires. During reassemble of the IP section, the wires may be stressed as the stainless tube was quite tight fitting, which introduced inhomogeneity in the wires. It was reported [6] that strain induced inhomogeneity in the Pt wire, which can be recovered by proper annealing. As the IP section of the thermocouples had some inhomogeneity, to get reproducible measured EMF at any fixed point, the immersion length of the IP section should need to be constant.

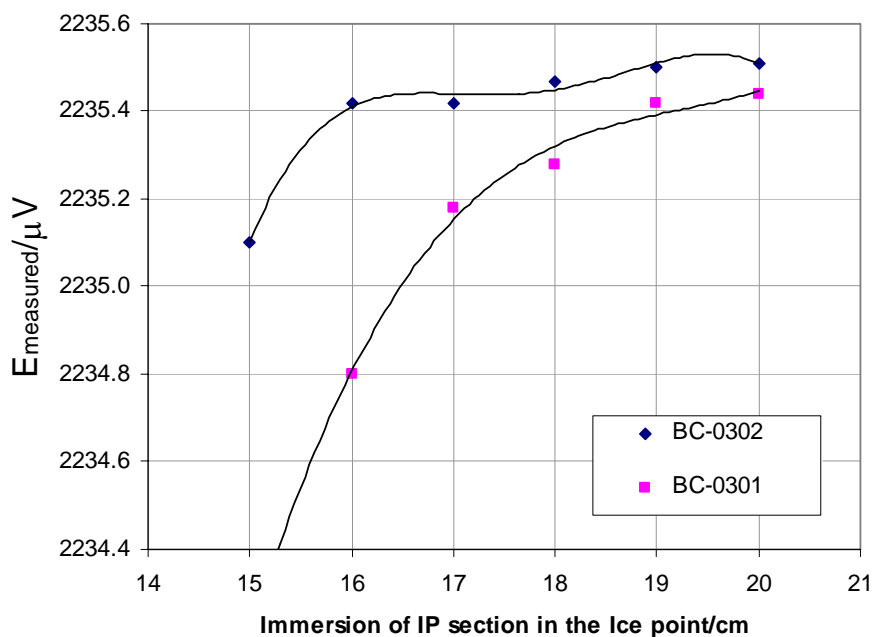


Fig. 8 Variation of measured EMF at the Sn point with the immersion length of the IP section in the ice point

## 6. Final Measurements by the Pilot Lab

Table 5 shows the final measurement results by the pilot laboratory. In addition to the fixed-point emf measurements, the dependence of the reference junction on the immersion depth into the ice bath was investigated at the Ga melting point to examine the possibility of damages in the reference junction. In table 6, the variation of the melting plateau emf with the immersion depth of the reference junction into the ice bath is shown. For BC-0301 thermocouple, the emf is changed about 0.2  $\mu\text{V}$  with withdrawal by 5 cm. But BC-0302 shows a variation of half of BC-0301. As noted by NMISA, the reference junction of BC-0301 seemed to be damaged more severely than BC-0302.

Fig.9 shows the inhomogeneity test results by the pilot laboratory after circulation. The immersion profiles seemed to be unchanged when compared with Fig.5.

Table 5. Measurement results at KRISS after circulation

Thermocouple	Emfs at fixed-points / $\mu\text{V}$				
	Ga	Sn	Zn	Al	Ag
BC-0301	$196.06 \pm 0.02$	$2235.82 \pm 0.03$	$4944.76 \pm 0.03$	$9318.24 \pm 0.04$	$16118.74 \pm 0.04$
	$196.02 \pm 0.02$	$2235.71 \pm 0.03$	$4944.61 \pm 0.03$	$9319.06 \pm 0.05$	$16118.84 \pm 0.02$
	$196.09 \pm 0.03$	$2235.70 \pm 0.03$	$4944.56 \pm 0.03$	$9319.25 \pm 0.05$	$16119.39 \pm 0.05$
	$196.06 \pm 0.04$	$2235.74 \pm 0.07$	$4944.64 \pm 0.10$	$9318.85 \pm 0.54$	$16118.99 \pm 0.35$
BC-0302	$196.05 \pm 0.03$	$2235.79 \pm 0.03$	$4944.67 \pm 0.03$	$9318.76 \pm 0.03$	$16118.44 \pm 0.04$
	$196.07 \pm 0.02$	$2235.88 \pm 0.04$	$4944.65 \pm 0.03$	$9318.86 \pm 0.03$	$16118.49 \pm 0.02$
	$196.04 \pm 0.02$	$2235.77 \pm 0.03$	$4944.58 \pm 0.03$	$9318.82 \pm 0.03$	$16118.73 \pm 0.02$
	$196.05 \pm 0.02$	$2235.81 \pm 0.06$	$4944.63 \pm 0.05$	$9318.81 \pm 0.05$	$16118.55 \pm 0.16$

Table 6. Immersion tests of the reference junction into the ice bath at the Ga point.

Immersion depth	BC-0301	BC-0302
Full immersion	196.06	196.05
Withdrawal by 3 cm	195.97	196.03
Withdrawal by 5 cm	195.86	195.96
Full immersion	196.06	196.07

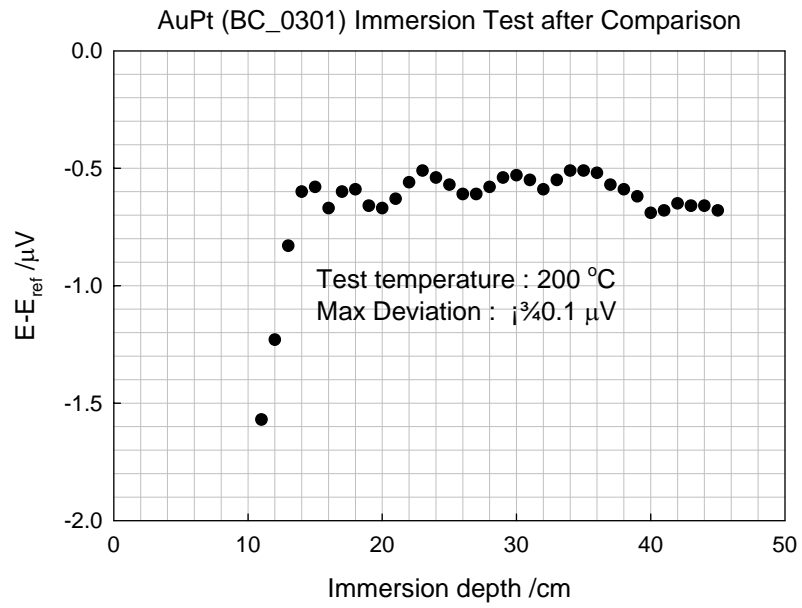


Fig.9 (a) Immersion result of BC-0301 by KRISS after circulation

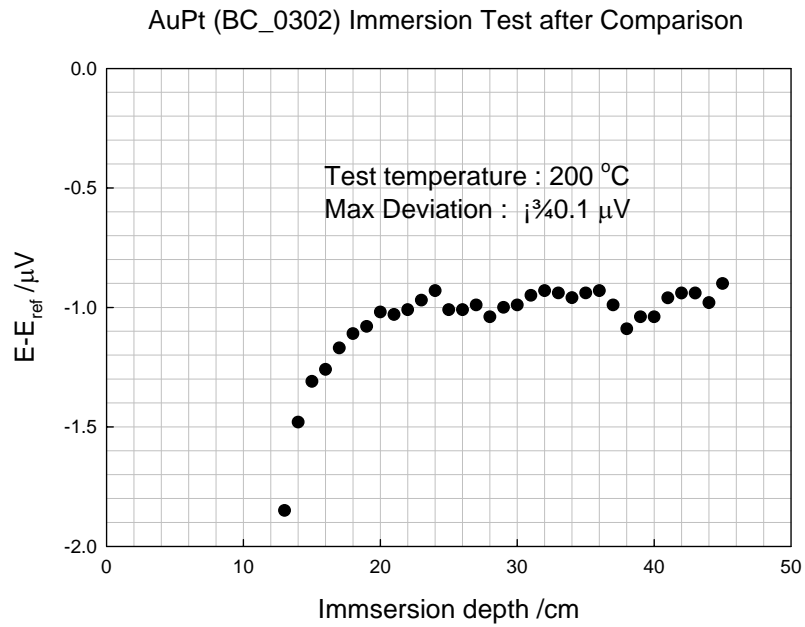


Fig.9 (b) Immersion result of BC-0302 by KRISS after circulation

Fig.10 shows the deviation of the emf values measured initially by KRISS from the reference function for two thermocouples. As indicated in the figure, deviation emfs at the Ag point showed a 1  $\mu\text{V}$  to 2  $\mu\text{V}$  deviation from the linear behavior extrapolated from the measurements at lower temperatures. The expected values from the extrapolation are much lower than the measured values. To investigate this abnormal behavior, thermocouples were tested using the same Ag cell in different furnaces.

In Table 7, measurement results are summarized. At different furnaces, thermocouples were tested 4 times separately using a same Ag cell. The average freezing emfs and standard deviation values are shown in the table. The two furnaces used in these tests have nearly same dimension and they are equipped with Na-heat pipes. At the FPF-M-01 furnace, the measured values were nearly same as the final measurement results using Ag-1 cell which was used for the comparison. However, at the FPF-H-02 furnace, the freezing emfs were lowered by 1.56  $\mu\text{V}$  for BC-0301 and 0.80  $\mu\text{V}$  for BC-0302 in average. These values were very close to the expected value shown in figure 10.

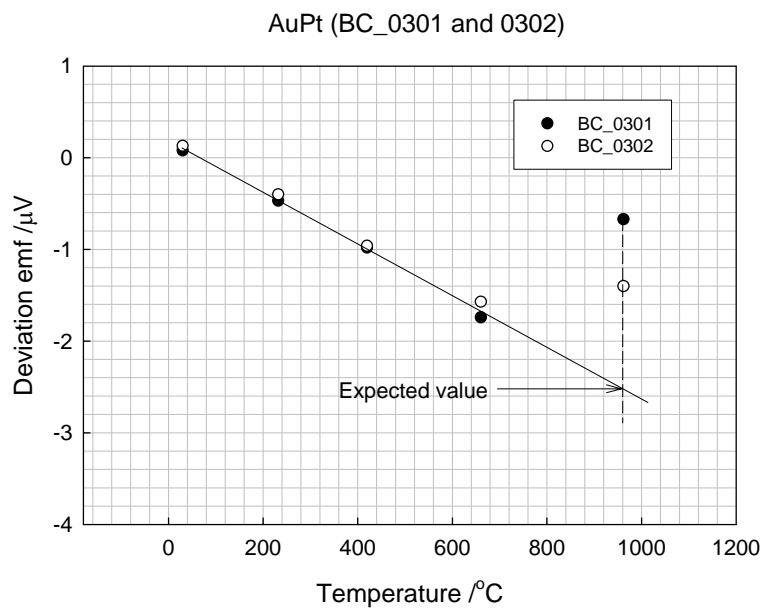


Fig.10 Deviation emfs of test thermocouples measured by KRISS before circulation

Table 7. Summary of the Ag fixed-point measurements at different furnace.

Furnace		FPF-H-02	FPF-M-01
Cell ID		LS-AG1	LS-AG1
TC	BC-0301	(16117.87 ± 0.16) $\mu\text{V}$	(16119.43 ± 0.29) $\mu\text{V}$
	BC-0302	(16117.67 ± 0.15) $\mu\text{V}$	(16118.47 ± 0.25) $\mu\text{V}$

Table 8. Measured resistance at the Ag freezing point in different furnaces.

Furnace	FPF-H-02	FPF-M-01
Read value ( $\pm 1 \sigma$ )	2.611 534 $\Omega$ ( $\pm 7.8 \times 10^{-7} \Omega$ )	2.611 540 $\Omega$ ( $\pm 7.3 \times 10^{-6} \Omega$ )
Difference	0.000 006 $\Omega$ ( $\sim 0.6$ mK)	

In order to examine these differences, the freezing temperature of LS-AG1 cell were investigated using a high temperature SPRT. The test HTSPRT was one from VNIIM (Model name: BTC, Serial number: N354) having a nominal resistance of 2.5  $\Omega$  at the triple point of water. Standard resistor from Tinsley having a nominal resistance of 25  $\Omega$  at 25  $^{\circ}\text{C}$  was used. A F18 bridge (S/N:1320 001 191) was used at the applied current of 5 mA with  $10^4$  gain. Table 8 shows the measured results, hereby the freezing conditions were same. The temperature difference was very small (about 0.6 mK), which was much smaller than the KRISS CMC value of the Ag freezing temperature. Therefore, it is found that freezing temperature of LS-AG1 cell is not dependent on the furnace used in the realization.

Since the thermocouple can be affected by the temperature gradient surrounding thermocouple wires, temperature gradients of two furnaces installed with Ag cell were measured at about 960  $^{\circ}\text{C}$  using Pt/Pd thermocouple. Fig. 11 shows temperature gradients along the immersion depth from the furnace top. FPF-H-02 furnace has slightly longer flat region by about 4 cm than that of FPF-M-01 furnace. It is not sure whether this small difference makes the apparent thermocouple emf difference shown in table 7.

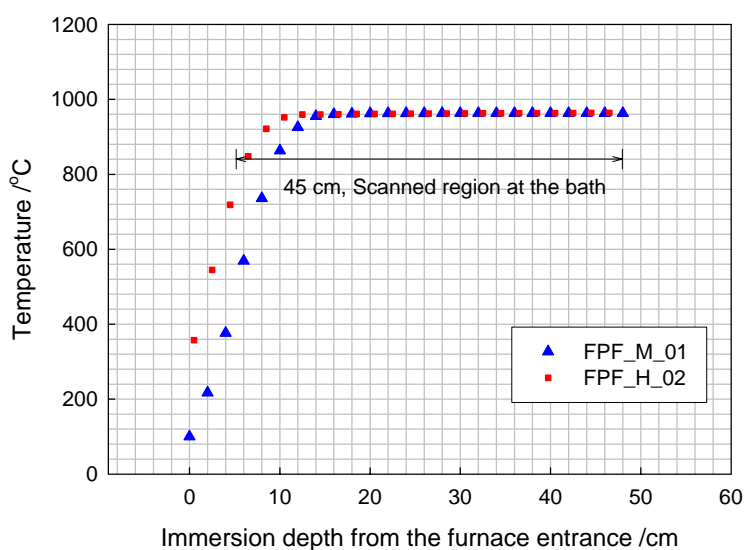


Fig 11. Temperature gradients of FPF-M-01 and FPF-H-02 furnace at 960  $^{\circ}\text{C}$ .

To examine the inhomogeneity profiles of test thermocouples in extended range up to 55 cm from the reference junction, they were sent to NMIA having a long range test facility. However, no distinguishable variation in the immersion profiles was found.

Even though many tests were performed to identify the origin of the difference in the freezing point emf values measured through Au/Pt thermocouples, it was failed to be explained explicitly. Nevertheless it is apparent that the Au/Pt test thermocouples show furnace dependence, so temperature gradient dependence.

**Thus it is provisionally concluded that the KRISS data at the Ag freezing point be corrected by amount of - 1.56  $\mu\text{V}$  for BC-0301 and - 0.80  $\mu\text{V}$  for BC-0302.**

## 7. Uncertainty evaluation

The calculated combined uncertainties are shown in Table 9 at each fixed-point. The details on each uncertainty terms are shown in appendix.

Inhomogeneity was calculated using equation (1).

$$\text{Inhomogeneity} = \Delta E / (E_{200\text{ }^\circ\text{C}} - E_{\text{RT}}) \times 100 \% \quad (1)$$

$\Delta E$  : maximum emf variation

$E_{200\text{ }^\circ\text{C}}$  : emf at 200  $^\circ\text{C}$

$E_{\text{RT}}$  : emf at room temperature

The standard uncertainty due to the inhomogeneity of thermocouple at each fixed points was calculated using equation (2).

$$u(x_i) = (E_{\text{measured}} - E_{\text{RT}}) \times \text{Inhomogeneity} / 100 \mu\text{V} \quad (3)$$

$E_{\text{measured}}$  : measured emf at fixed-point

### **KRISS :**

The uncertainty of BC-0301 after circulation shows the largest value. Thus the presented uncertainty values are for this measurement. The repeatability is calculated from the standard deviation of the mean of three measurements. The calibration uncertainty of the voltmeter used in comparison is 10  $\mu\text{V}/\text{V}$  ( $k = 2$ ), and the manufacturer's long term accuracy is 20  $\mu\text{V}/\text{V}$  ( $k = 2$ ) of reading. The inhomogeneity is calculated from the maximum variation in emf from 100 mm to 450 mm immersion as the full width of a rectangular distribution. Especially at the Ag point, the temperature gradient effect is considered and the pooled standard deviation of 4 measurements at two difference furnaces is used.

### **NMISA :**

Uncertainty analyses at all points are for BC-0302 having larger inhomogeneity. At all points, uncertainty of BC-0302 is larger than that of BC-0301. The repeatability is calculated from the standard deviation of the mean of three measurements. The calibration uncertainty of the voltmeter used in comparison is 34  $\mu\text{V}/\text{V}$  ( $k = 2$ ), and the uncertainty due to drift is [80  $\mu\text{V}/\text{V}$  of reading + 12  $\mu\text{V}/\text{V}$  of range] ( $k = 1.732$ ). The inhomogeneity is calculated from the maximum variation in emf from 130 mm to 420 mm immersion

as the full width of a rectangular distribution: reduced to a standard uncertainty ( $k = 1$ ), this component is 0.006 %.

**NMIA :**

The repeatability is calculated from the standard deviation of five measurements. The calibration uncertainty of the voltmeter used in comparison is  $2 \mu\text{V/V}$  ( $k = 2$ ), and the one year stability is  $22 \mu\text{V/V}$  ( $k = 2$ ) of reading. The inhomogeneity is calculated to be 0.006 % ( $k = 2$ ).

Table 9. Combined standard uncertainties ( $u_c$ ) at each fixed-point in  $\mu\text{V}$ .

	Ga	Sn	Zn	Al	Ag
KRISS	0.06	0.11	0.20	0.47	0.66
NMISA	0.25	0.36	0.55	0.87	1.41
NMIA	0.05	0.08	0.13	0.26	0.50

8. Comparison Data Analysis

Table 10 and 11 shows the measured emfs at each participant and the maximum differences between participants. In the parentheses, maximum emf difference is converted to the temperature unit. KRISS data at Ag point are corrected values. In this comparison, the comparison reference value is not calculated since the number of participants is too small. At the Ga point, maximum deviation is as large as 60 mK for BC-0301. At higher temperatures, temperature differences are 10 mK to 40 mK. Thus it is concluded that temperature scale of the Au/Pt thermocouple between three NMIs is coincided within 60 mK from Ga to Ag point.

Table 10. Fixed-point emfs and the maximum differences of the BC\_0301 in  $\mu\text{V}$ .

NMIs	KRISS <sub>B</sub>	NMISA	NMIA	KRISS <sub>A</sub>	Max. difference
Ga	196.34	195.90	196.02	196.06	0.44 $\mu\text{V}$ (0.06 °C)
Sn	2235.71	2235.34	2235.38	2235.74	0.40 $\mu\text{V}$ (0.03 °C)
Zn	4944.65	4944.35	4944.31	4944.67	0.36 $\mu\text{V}$ (0.02 °C)
Al	9318.70	9318.60	9318.33	9318.85	0.52 $\mu\text{V}$ (0.03 °C)
Ag	16118.27	16117.90	16117.36	16117.43	0.91 $\mu\text{V}$ (0.04 °C)

Table 11. Fixed-point emfs and the maximum differences of the BC\_0302 in  $\mu\text{V}$ .

NMIs	KRISS <sub>B</sub>	NMISA	NMIA	KRISS <sub>A</sub>	Max. difference
Ga	196.39	196.09	196.10	196.05	0.34 $\mu\text{V}$ (0.05 °C)
Sn	2235.78	2235.61	2235.46	2235.81	0.35 $\mu\text{V}$ (0.03 °C)
Zn	4944.61	4944.35	4944.39	4944.63	0.28 $\mu\text{V}$ (0.02 °C)
Al	9318.87	9318.89	9318.69	9318.81	0.20 $\mu\text{V}$ (0.01 °C)
Ag	16118.30	16118.15	16117.34	16117.75	0.96 $\mu\text{V}$ (0.04 °C)

Fig.12 shows the plots of deviation emfs from the reference function [1] at each fixed-point. KRISS data are after the correction. Deviation emfs data show linear dependencies on temperature. After circulation, emfs at Ga and Ag points decreased for both thermocouples. But at other points, emfs values seemed unchanged. In Figs.13 to 17, emf values at each fixed points are shown with error bars (combined standard uncertainties).

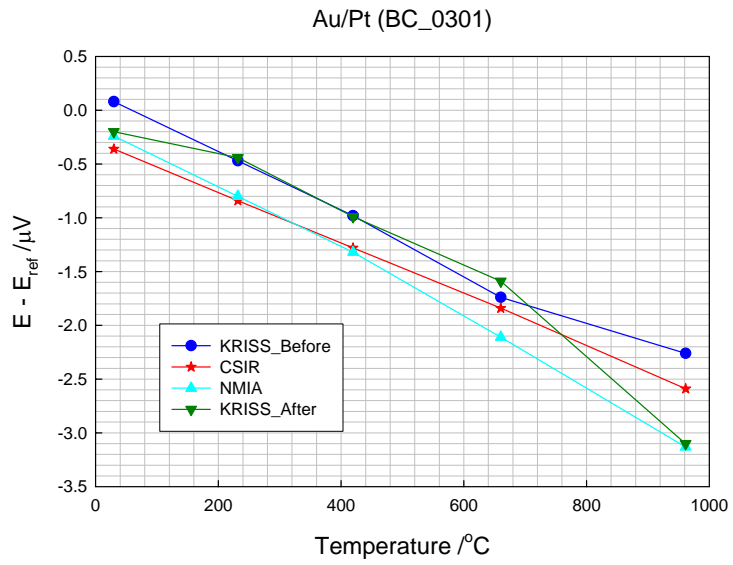


Fig.12 (a) Plots of deviation emfs at fixed-points with temperature for BC-0301

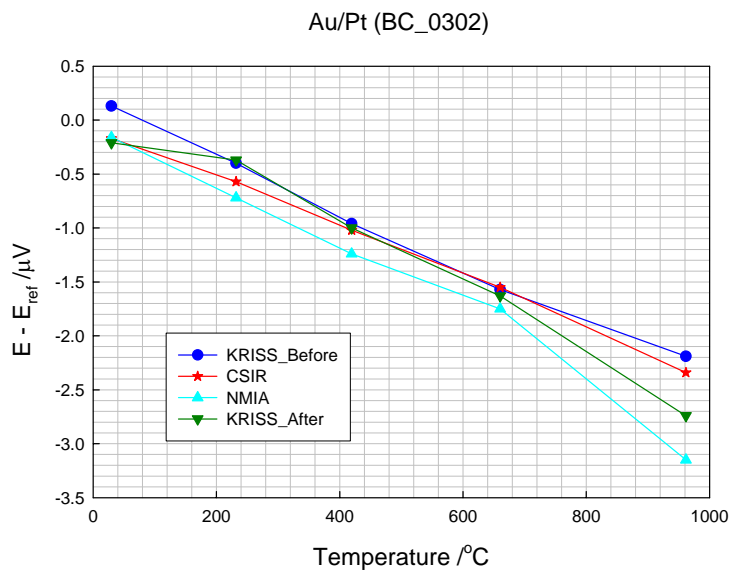


Fig.12 (b) Plots of deviation emfs at fixed-points with temperature for BC-0302

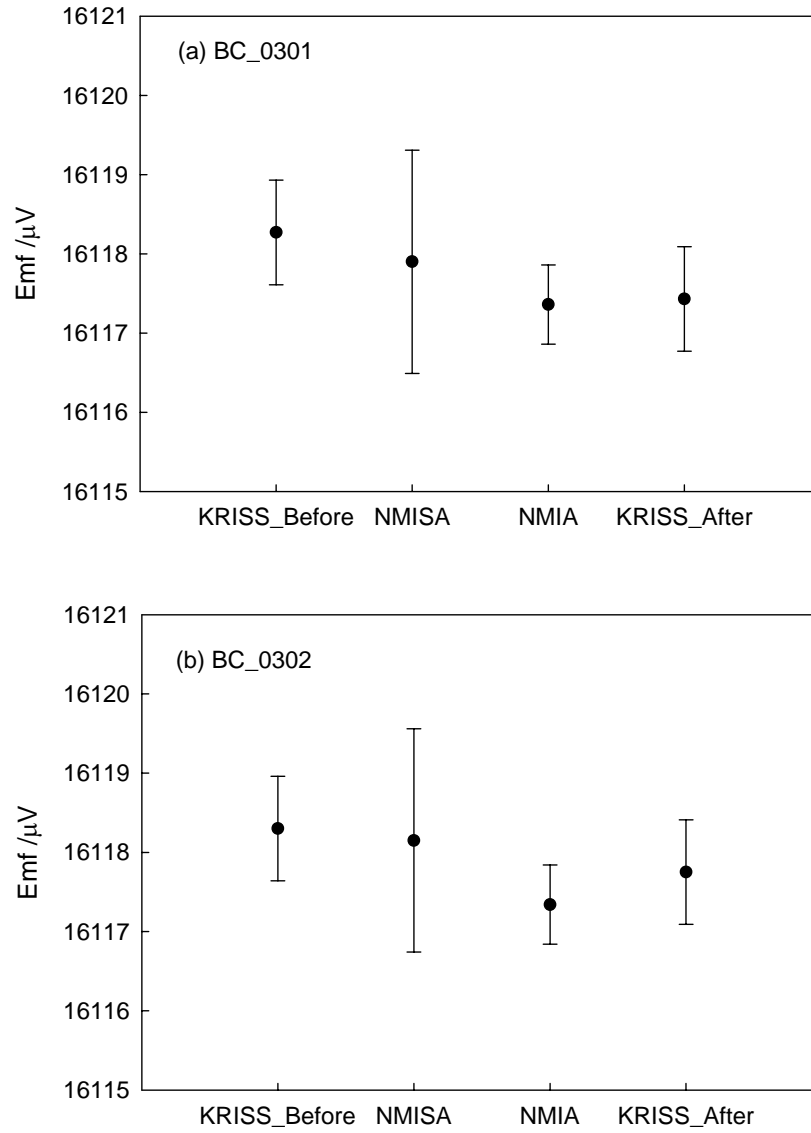


Fig.13. Emfs at Ag points. Error bar denotes the combined standard uncertainty.

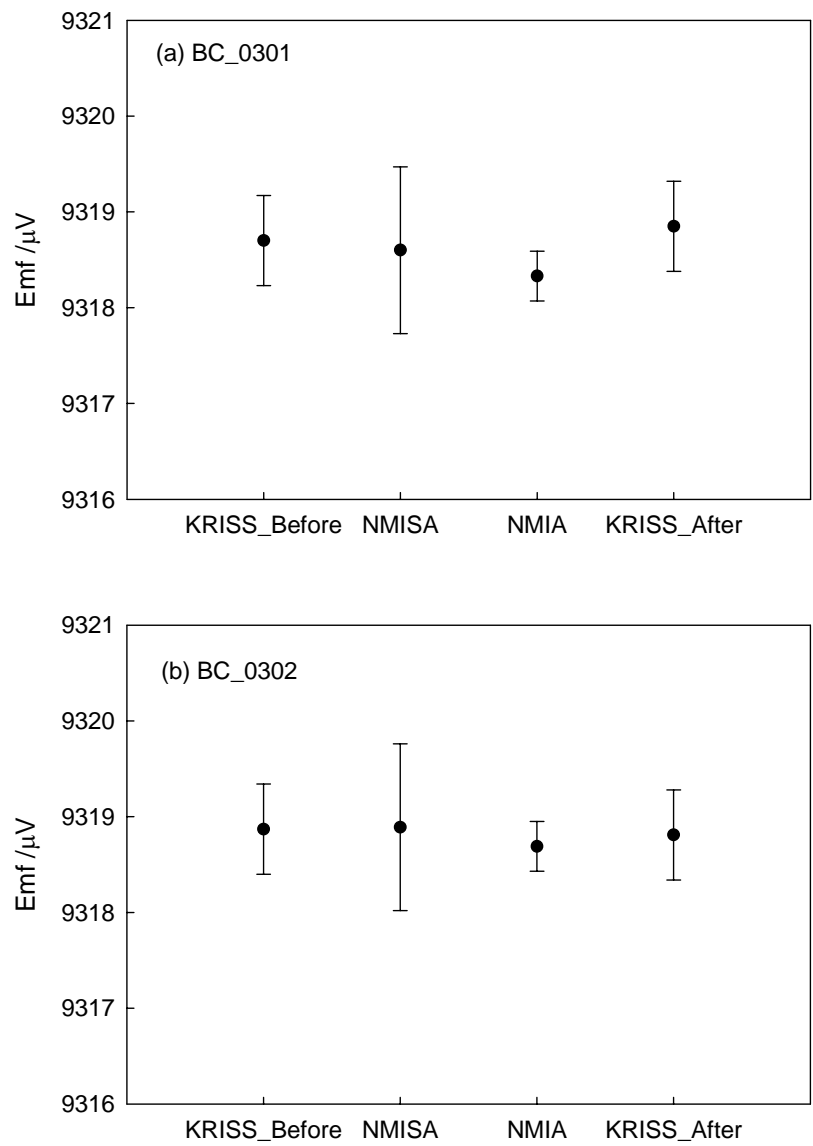


Fig.14. Emfs at Al points. Error bar denotes the combined standard uncertainty.

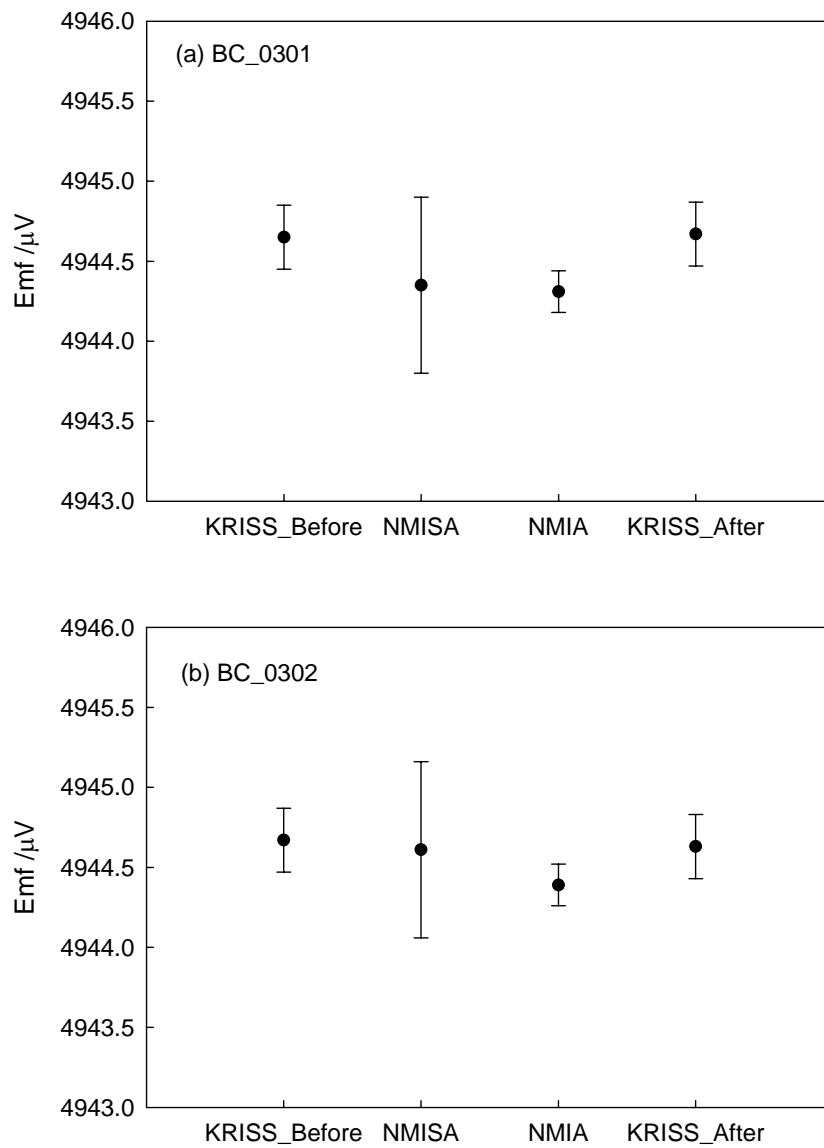


Fig.15. Emfs at Zn points. Error bar denotes the combined standard uncertainty.

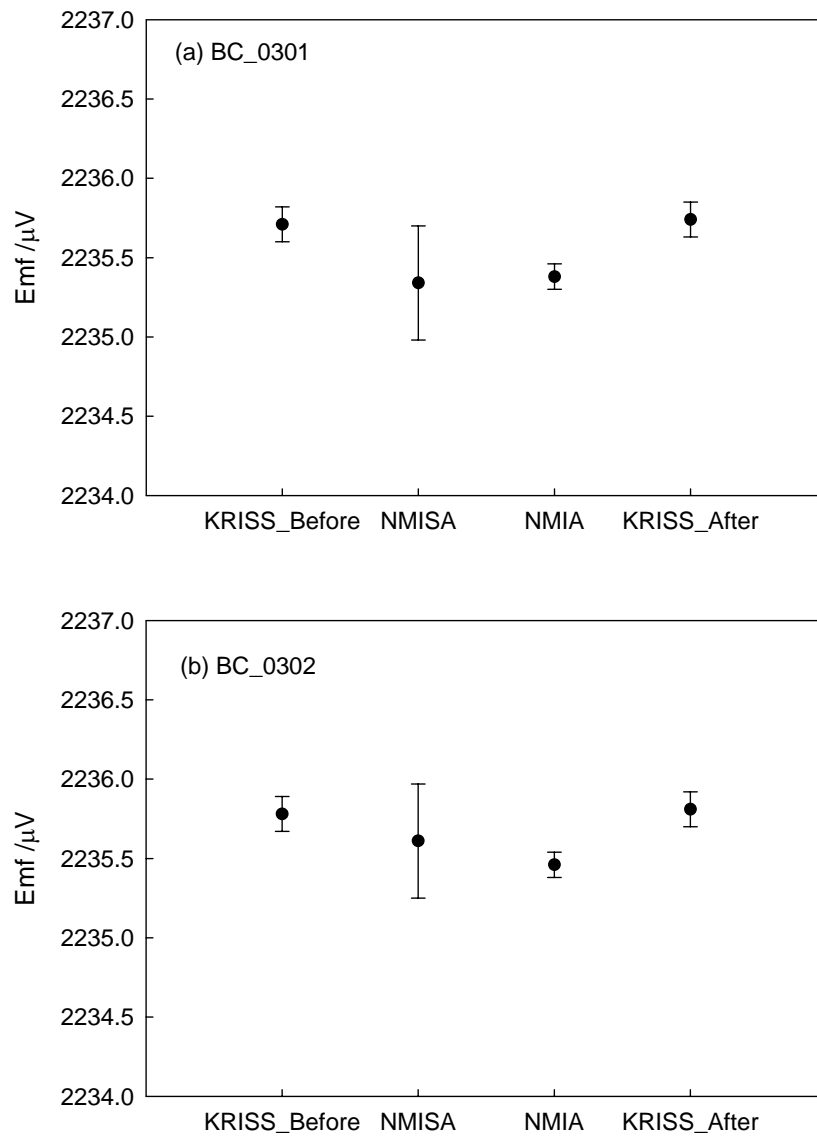


Fig.16. Emfs at Sn points. Error bar denotes the combined standard uncertainty.

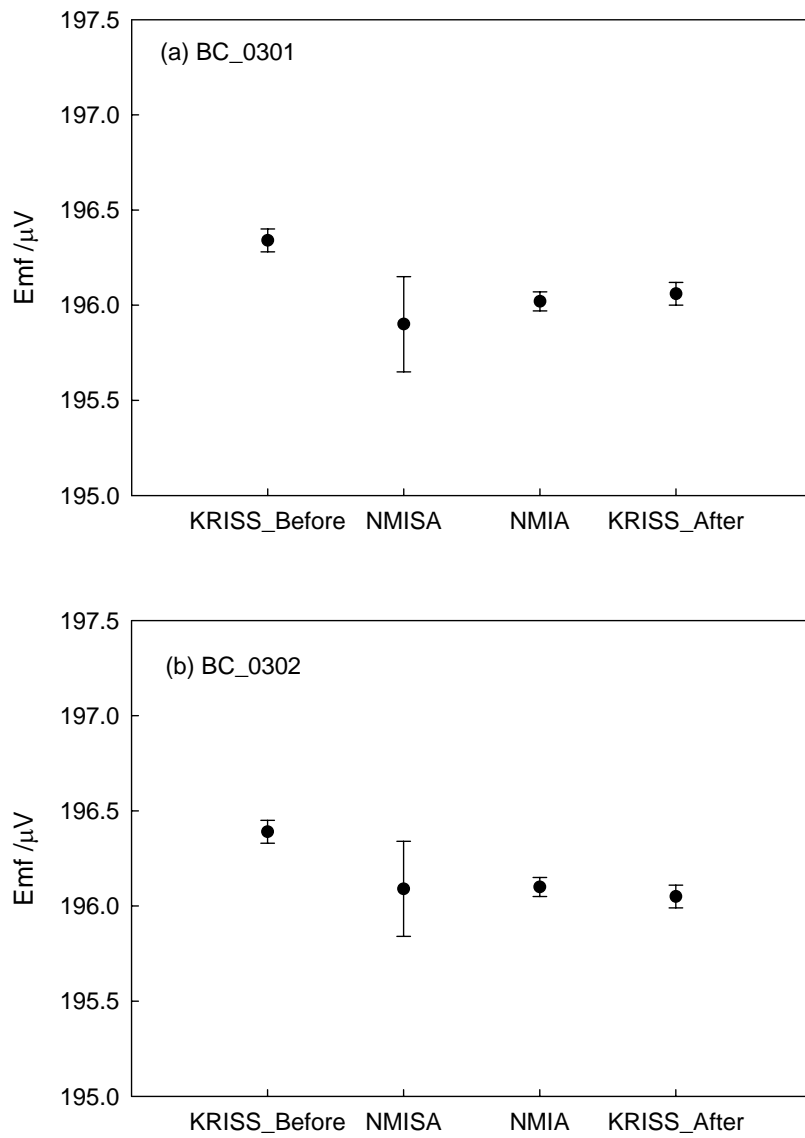


Fig.17. Emfs at Ga points. Error bar denotes the combined standard uncertainty.

## 9. References

- [1] ASTM E1751-2000, "Standard Guide for Temperature Electromotive Force (EMF) Tables for Non-Letter Designated Thermocouple Combinations

# Protocol for Fixed-Point Comparison of Au/Pt thermocouples

April 10, 2003

Y.-G. Kim

Korea Research Institute of Standards and Science  
P.O.Box 102 Yuseong, Daejeon 305-600, Republic of Korea

## INTRODUCTION

This regional comparison was initiated during 2002 Temperature symposium in October, 2002 by KRISS, NMIA and NMISA. KRISS was invited to be the pilot laboratory of this comparison. The procedures and instructions, which are given below, should be followed by the participants. Two Au/Pt thermocouples provided by KRISS will be used as transfer thermometers. The Au/Pt thermocouple should be compared from Ga to Ag.

## LIST of PARTICIPANTS

KRISS            Yong-Gyoo Kim, Temperature-Humidity Group,  
(Korea)            [dragon@kriss.re.kr](mailto:dragon@kriss.re.kr)

NMIA            Ferdouse Jahan, Thermometry group,  
(Australia)        [Ferdouse.Jahan@measurement.gov.au](mailto:Ferdouse.Jahan@measurement.gov.au)

NMISA            Hans Liedberg, Temperature Laboratory,  
(South Africa)    [hliedber@nmisa.org](mailto:hliedber@nmisa.org)

## APPARATUS

1. All participating laboratory must have Ga, Sn, Zn, Al, and Ag freezing-point cells whose thermometer wells have inner diameter larger than 8 mm.
2. All participating laboratory should have the annealing furnace in vertical type whose immersion depth should be longer than 50 cm and operating temperature should be high to 1100 °C.
3. All participating laboratory should prepare the thermocouple inhomogeneity test system operating at 150 °C ~ 200 °C. Its immersion depth should be longer than 40 cm. It is recommended that the test temperature is 200 °C.
4. All participating laboratory should have a precise digital voltmeter having a resolution of 0.01  $\mu$ V.

## SCHEDULE

The following schedule applies for all participants being in charge to transport the transfer thermometers to the next participating laboratory. The transfer standards can be carried by air-mail in their case to next participating laboratory. Each laboratory should complete the measurement within approximately one month.

March, 2003	Fabrication of transfer standards by KRISS Measurements completed
April, 2003	Moved to NMISA by air mail Measurements completed
May, 2003	Moved to NMIA by air mail Measurements completed
June, 2003	Moved to KRISS by hand-carry Final measurements
July, 2003	Completion of the comparison and Preparation of the comparison report
August, 2003	Submit the report to APMP

## DETAILED INSTRUCTIONS FOR PARTICIPATING LABORATORIES

### Remarks

Each participant should follow the instructions given in (B) (Receiving the Thermometers) as soon as possible after receiving the thermometers. After this, calibrate the specified thermometers through the given procedures at each fixed-point. After the calibrations, pack securely the thermometers and transport them to the next participant. If any discussion on this protocol is necessary, the participant should share the information through e-mail to all participants.

### (A) Preparation of standard thermocouples

#### Procedures

1. KRISS should make two set of Au/Pt thermocouples as transfer standard. KRISS should provide the preparation method to participants in detail.
2. KRISS should present the source of the thermocouple wires and their nominal purities.
3. KRISS should present the annealing temperature and time spent.

### (B) Receiving the Thermometers

#### Procedures

1. Upon receiving the transfer thermocouples, the host laboratory must inspect them for damage. The host laboratory must report the condition of the thermocouples to the KRISS. If there is damage, KRISS will give instructions on how to proceed.
2. If there is no damage, the host must anneal them at 1000 °C for 1 h before measurement in order to eliminate the stress which would be caused during transfer. The temperature profile of the annealing furnace should be examined before inserting the thermocouples. The temperature profile should be checked from the furnace surface to its maximum immersion depth with an interval of 2 cm .
3. After annealing, pull out the thermocouple to ambient rapidly in order to prohibit the oxidation of Pt.

### (C) Calibration of Au/Pt thermocouples at the Ga, Sn, Zn, Al and Ag fixed-points

#### Remarks

Au/Pt thermocouples should be calibrated at the Ga, Sn, Zn, Al and Ag points. The realization sequence is from high temperature to low temperature. The general procedures are referred to Supplementary information of the ITS-90.

#### Procedures

1. Before measurement at the freezing points, the temperature profile of the enclosure should be examined from the bottom of the cell to the enclosure surface (5°C below the melting temperature except for Ga). It is recommended to use another Au/Pt or Pt/Pd thermocouple as a measuring sensor (SPRT can be used also).
2. Insert the monitoring thermocouple(thermometer) into the freezing cell. During melting, record the melting emf of the monitoring thermocouple. After completion of melting, let the melt stabilize at 2 °C above freezing temperature. And then cool down to 5 °C below freezing temperature with a cooling rate of 0.5 °C/min. If the temperature increases after supercool, ramp the furnace set temperature to 1°C ~ 2 °C below the freezing temperature.
3. Remove the monitoring thermocouple and insert the cool quartz rod for 2 min. This chill rod induce will make a flat freezing plateau. After removing the quartz rod, insert the test thermocouple (S/N : BC\_0301) into the cell and monitor its thermal emf. It is highly recommended to use the computer-interfaced data logging system. The participants should record the emf for about 30 min.
4. Replace the test thermocouple with another Au/Pt (S/N : BC\_0302) followed by about 30 min measurement. After measurement, cool down the furnace 20 °C below the freezing temperature. And then let the melt freeze completely. The test thermocouple should be removed from the cell, and the monitoring thermocouple used to record the next melt and supercool. The participants should repeat the realization 3 times at each fixed point.
5. In next realization, insert at first BC\_0302 thermocouple and then BC\_0301.
6. In third realization, get the freezing curve about 1 h for each thermocouple. After final measurement, remove the test thermocouple from the furnace to ambient rapidly.
7. In case of Ga realization, it is not necessary to use the monitoring thermocouple. It is recommended that the set temperature to melt is 1 °C above the melting temperature.
8. After completion of the fixed-point measurements, Au/Pt thermocouples should be tested at the inhomogeneity test system operating at 200 °C. Inhomogeneity test should be conducted during insertion process. The test length should be larger than 40 cm from the tip of the thermocouple. This inhomogeneity test should be conducted three times.

## REPORT OF RESULTS

The participating laboratories must send the followings to the all participants.

1. Information on the measuring devices. Please fill the Table 1 in appendix.
2. Information on the inhomogeneity test system. Please fill the Table 2 in appendix.
3. Graphs of furnace temperature gradient and their data.
4. The measurement data and their electronic files. Please fill the Table 3 in appendix.
5. Uncertainty analysis according to the "Guide to the Expression of Uncertainty in Measurement", ISO 1993, ISBN 92-67-10188-9. The emf across the test thermocouple at the fixed-point can be written as equation (A1). Please fill the Table 4 in appendix.

$$E_x(t_x) = E(t_F) + (\delta t_F + \delta t_{HF})C_F + \delta E_{VC} + \delta E_{VR} + \delta E_{VD} + \delta E_{SC} + \delta t_0 C_0 + \delta E_{IH} + \delta E_{EN} \quad (A1)$$

$E(t_F)$  : Emf at the fixed-point temperature (Type A)

$\delta t_F$  : Correction due to the fixed-point calibration

$\delta t_{HF}$  : Correction due to the heat loss through the thermocouple sheath

$C_F$  : Sensitivity at the fixed-point ( $\mu V/^\circ C$ )

$\delta E_{VC}$  : Correction due to the voltmeter calibration

$\delta E_{VR}$  : Correction due to the voltmeter resolution

$\delta E_{VD}$  : Correction due to the voltmeter drift (long term accuracy in manual)

$\delta E_{SC}$  : Correction due to the scanner (if used)

$\delta t_0$  : Correction due to the ice temperature (Please use the measurement result.)

$C_0$  : Sensitivity at the ice temperature ( $\mu V/^\circ C$ )

$\delta E_{IH}$  : Correction due to the inhomogeneity (Please use the measurement result.)

$\delta E_{EN}$  : Correction due to the electric noise

Table 1. Information on the measuring devices used in this comparison

Devices		Manufacturer	Model(Type)	S/N	Remarks
DMM					
Ice point					
Scanner (if used)					
Ag	Cell				
	Enclosure				
Al	Cell				
	Enclosure				
Zn	Cell				
	Enclosure				
Sn	Cell				
	Enclosure				
Ga	Cell				
	Enclosure				

Table 2. Information on the inhomogeneity test system

Items	
Measuring DMM	
Temperature enclosure	
Scanning method	
Reference thermometer (if used)	
Test temperature	
Stability	

Table 3. Measurement data

Fixed-point	Mean value for 10 min $\pm$ standard deviation <sup>1)</sup>		File names <sup>2)</sup>
	AuPt1	AuPt2	
Ag	Data 1	Data 1	
	Data 2	Data 2	
	Data 3	Data 3	
Al	Data 1	Data 1	
	Data 2	Data 2	
	Data 3	Data 3	
Zn	Data 1	Data 1	
	Data 2	Data 2	
	Data 3	Data 3	
Sn	Data 1	Data 1	
	Data 2	Data 2	
	Data 3	Data 3	
Ga	Data 1	Data 1	
	Data 2	Data 2	
	Data 3	Data 3	

1) Mean values for last 10 min in  $\mu\text{V}$     2) NMI name-Fixed Point-t/c ID-run number.txt

Table 4. Uncertainty analysis sheet

Quantity $X_i$	Estimate $x_i$	Standard uncertainty $u(x_i)$	Probability distribution	Sensitivity coefficient $c_i$	Uncertainty contribution $u_i(y)$	Degree of freedom
$E_F$						
$\delta t_F$						
$\delta t_{HF}$						
$\delta E_{VC}$						
$\delta E_{VR}$						
$\delta E_{VD}$						
$\delta E_{SC}$						
$\delta t_0$						
$\delta E_{IH}$						
$\delta E_{EN}$						
$E_x$						

## Appendix B. Description of the measuring devices of participants

Table A-1. Information on the measuring devices used in this comparison of KRISS

Devices	Manufacturer	Model(Type)	S/N	Remarks	
DMM	Keithley	2182			
Ice point	KRISS-made	Water + ice	-	Distilled water	
Scanner (if used)	Not used		-		
Ag	Cell	KRISS-made	Sealed	AG-1	-
	Enclosure	KRISS-made	Na heat-pipe furnace	FPF-AG-1	One zone
Al	Cell	KRISS-made	Sealed	AL-1	-
	Enclosure	KRISS-made	Na heat-pipe furnace	FPF-AL-1	One zone
Zn	Cell	KRISS-made	Sealed	ZN-1	-
	Enclosure	ISOTECH	17703	ISOF-ZN-1	Three zone
Sn	Cell	KRISS-made	Sealed	SN-1	-
	Enclosure	ISOTECH	17703	ISOF-ZN-1	Three zone
Ga	Cell	ISOTECH	ITL-M-17401	131	Teflon crucible
	Enclosure	ISOTECH	ITL-M-17402B	BA-GA-2	Peltier cooler

Table A-2. Information on the inhomogeneity test system of KRISS

Items	Description
Measuring DMM	Keithley DMM 2001
Temperature enclosure	Hart Liquid Bath Model 6022 Maximum immersion depth of 450 mm
Scanning method	Manual scanning with 2 cm interval
Reference thermometer (if used)	ASL F700 with SPRT (Rosemount 162CE)
Test temperature	200 °C
Stability	Below 5 mK

Table A-3. Information on the measuring devices used in this comparison of NMISA

Devices	Manufacturer	Model(Type)	S/N	Remarks	
DVM	Keithley	182	0552803	-48 ppm drift Feb-Jun 2003: corrected by linear interpol.	
Ice point	NMISA-made	Water + ice		Distilled water	
Scanner (if used)	Keithley	705 + 7059 low-voltage card	521077		
Ag	Cell	Isotech	Sealed	AG36	
	Enclosure	Isotech	17705 Na heat-pipe furnace	161371/1	One zone
Al	Cell	Isotech	Sealed	AL108	
	Enclosure	Isotech	17705 Na heat-pipe furnace	161371/1	One zone
Zn	Cell	Isotech	Sealed	ZN118	
	Enclosure	Isotech	875 fluidised bath	161371/3	One zone
Sn	Cell	Isotech	Sealed	SN77	
	Enclosure	Isotech	875 fluidised bath	161371/3	One zone
Ga	Cell	NMISA-made	Sealed	TS-010	Teflon crucible
	Enclosure	Heto	CB216 water bath	8009436	

Table A-4. Information on the inhomogeneity test system of NMISA

Items	Description
Measuring DMM	Keithley 182 DVM
Temperature enclosure	Isotech liquid bath model 915 Maximum immersion depth of 425 mm
Scanning method	Manual scanning with 2 to 3 cm interval
Reference thermometer (if used)	ASL F18 with SPRT (L&N 8167-25)
Test temperature	200.2 °C
Stability	Std deviation of SPRT at one depth $\leq$ 12 mK

Table A-5. Information on the measuring devices used in this comparison of NMIA

Devices	Manufacturer	Model(Type)	S/N	Remarks
DMM	Agilent	34420A	US28028724	High accuracy option
Ice point	NMI-made	Water + ice	-	Distilled water
Scanner (if used)	No	N/A		
Ag	Cell	NMI-made	Open	-
	Enclosure	NMI-made	furnace	Three zone
Al	Cell	NMI-made	Open	-
	Enclosure	NMI-made	furnace	Three zone
Zn	Cell	NMI-made	Open	-
	Enclosure	NMI-made	furnace	Three zone
Sn	Cell	NMI-made	Open	-
	Enclosure	NMI-made	furnace	Three zone
Ga	Cell	YSI	Open	Teflon crucible
	Enclosure	YSI	furnace	

Table A-6. Information on the inhomogeneity test system of NMIA

Items	Description
Measuring DMM	HP 3458A DMM
Temperature enclosure	NMI made Oil Bath Maximum immersion depth of 650 mm
Scanning method	Step motor driven Scanning speed of 100 mm/hour Computer-interfaced automatic operation system
Reference thermometer (if used)	No
Test temperature	200 °C
Stability	Below 10 mK

## Appendix C. Uncertainty Evaluation Tables

Table A-7. Uncertainty analysis at Ag point (BC\_0301 after circulation) of KRISS

Quantity $X_i$	Estimate $x_i$	Standard uncertainty $u(x_i)$	Probability distribution	Sensitivity coefficient $c_i$	Uncertainty contribution $u_i(y) / \mu\text{V}$	Degree of freedom
$E_F$	16118.95	0.20 $\mu\text{V}$	Normal (k=1)	1	0.20	2
$\delta t_F$		0.01 $^{\circ}\text{C}$	Rectangular	24.95 $\mu\text{V}/^{\circ}\text{C}$	0.14	$\infty$
$\delta t_{HF}$		0.005 $^{\circ}\text{C}$	Rectangular	24.95 $\mu\text{V}/^{\circ}\text{C}$	0.07	$\infty$
$\delta E_{VC}$		0.08 $\mu\text{V}$	Normal (k=1)	1	0.08	$\infty$
$\delta E_{VR}$		0.005 $\mu\text{V}$	Rectangular	1	0.003	$\infty$
$\delta E_{VD}$		0.33 $\mu\text{V}$	Rectangular	1	0.19	$\infty$
$\delta E_{SC}$		-	-	-	-	-
$\delta t_0$		0.01 $^{\circ}\text{C}$	Rectangular	6.03 $\mu\text{V}/^{\circ}\text{C}$	0.04	$\infty$
$\delta E_{IH}$		0.006 %	Rectangular	1	0.55	$\infty$
$\delta E_{EN}$		0.01 $\mu\text{V}$	Rectangular	1	0.006	$\infty$
$\delta E_{FD}^*$	-1.56	0.13 $\mu\text{V}$	Normal (k=1)	1	0.13	5
$E_x$	16118.23				<b>0.66</b>	$\gg 500$

(\* $\delta E_{FD}$ : Correction due to the furnace dependence. Only apply to the silver point)

Table A-8. Uncertainty analysis at Al point (BC\_0301 after circulation) of KRISS

Quantity $X_i$	Estimate $x_i$	Standard uncertainty $u(x_i)$	Probability distribution	Sensitivity coefficient $c_i$	Uncertainty contribution $u_i(y) / \mu\text{V}$	Degree of freedom
$E_F$	9318.85	0.31 $\mu\text{V}$	Normal (k=1)	1	0.31	2
$\delta t_F$		0.005 $^{\circ}\text{C}$	Rectangular	20.14 $\mu\text{V}/^{\circ}\text{C}$	0.06	$\infty$
$\delta t_{HF}$		0.005 $^{\circ}\text{C}$	Rectangular	20.14 $\mu\text{V}/^{\circ}\text{C}$	0.06	$\infty$
$\delta E_{VC}$		0.05 $\mu\text{V}$	Normal (k=1)	1	0.05	$\infty$
$\delta E_{VR}$		0.005 $\mu\text{V}$	Rectangular	1	0.003	$\infty$
$\delta E_{VD}$		0.19 $\mu\text{V}$	Rectangular	1	0.11	$\infty$
$\delta E_{SC}$		-	-	-	-	-
$\delta t_0$		0.01 $^{\circ}\text{C}$	Rectangular	6.03 $\mu\text{V}/^{\circ}\text{C}$	0.04	$\infty$
$\delta E_{IH}$		0.006 %	Rectangular	1	0.32	$\infty$
$\delta E_{EN}$		0.01 $\mu\text{V}$	Rectangular	1	0.006	$\infty$
$E_x$	9318.85				<b>0.48</b>	$\gg 500$

Table A-9. Uncertainty analysis at Zn point (BC\_0301 after circulation) of KRISS

Quantity $X_i$	Estimate $x_i$	Standard uncertainty $u(x_i)$	Probability distribution	Sensitivity coefficient $c_i$	Uncertainty contribution $u_i(y) / \mu\text{V}$	Degree of freedom
$E_F$	4944.64	0.06 $\mu\text{V}$	Normal (k=1)	1	0.06	2
$\delta t_F$		0.005 $^{\circ}\text{C}$	Rectangular	16.16 $\mu\text{V}/^{\circ}\text{C}$	0.05	$\infty$
$\delta t_{HF}$		0.005 $^{\circ}\text{C}$	Rectangular	16.16 $\mu\text{V}/^{\circ}\text{C}$	0.05	$\infty$
$\delta E_{VC}$		0.02 $\mu\text{V}$	Normal (k=1)	1	0.02	$\infty$
$\delta E_{VR}$		0.005 $\mu\text{V}$	Rectangular	1	0.003	$\infty$
$\delta E_{VD}$		0.10 $\mu\text{V}$	Rectangular	1	0.06	$\infty$
$\delta E_{SC}$		-	-	-	-	-
$\delta t_0$		0.01 $^{\circ}\text{C}$	Rectangular	6.03 $\mu\text{V}/^{\circ}\text{C}$	0.04	$\infty$
$\delta E_{IH}$		0.006 %	Rectangular	1	0.17	$\infty$
$\delta E_{EN}$		0.01 $\mu\text{V}$	Rectangular	1	0.006	$\infty$
$E_x$	4944.64				<b>0.20</b>	$\gg 500$

Table A-10. Uncertainty analysis at Sn point (BC\_0301 after circulation) of KRISS

Quantity $X_i$	Estimate $x_i$	Standard uncertainty $u(x_i)$	Probability distribution	Sensitivity coefficient $c_i$	Uncertainty contribution $u_i(y) / \mu\text{V}$	Degree of freedom
$E_F$	2235.74	0.04 $\mu\text{V}$	Normal (k=1)	1	0.04	2
$\delta t_F$		0.005 $^{\circ}\text{C}$	Rectangular	12.6 $\mu\text{V}/^{\circ}\text{C}$	0.04	$\infty$
$\delta t_{HF}$		0.005 $^{\circ}\text{C}$	Rectangular	12.6 $\mu\text{V}/^{\circ}\text{C}$	0.04	$\infty$
$\delta E_{VC}$		0.05 $\mu\text{V}$	Normal (k=1)	1	0.01	$\infty$
$\delta E_{VR}$		0.005 $\mu\text{V}$	Rectangular	1	0.003	$\infty$
$\delta E_{VD}$		0.05 $\mu\text{V}$	Rectangular	1	0.03	$\infty$
$\delta E_{SC}$		-	-	-	-	-
$\delta t_0$		0.01 $^{\circ}\text{C}$	Rectangular	6.03 $\mu\text{V}/^{\circ}\text{C}$	0.04	$\infty$
$\delta E_{IH}$		0.006 %	Rectangular	1	0.07	$\infty$
$\delta E_{EN}$		0.01 $\mu\text{V}$	Rectangular	1	0.006	$\infty$
$E_x$	2235.74				<b>0.11</b>	$\gg 500$

Table A-11. Uncertainty analysis at Ga point (BC\_0301 after circulation) of KRISS

Quantity $X_i$	Estimate $x_i$	Standard uncertainty $u(x_i)$	Probability distribution	Sensitivity coefficient $c_i$	Uncertainty contribution $u_i(y) / \mu\text{V}$	Degree of freedom
$E_F$	196.06	0.03 $\mu\text{V}$	Normal (k =1)	1	0.03	2
$\delta t_F$		0.005 $^{\circ}\text{C}$	Rectangular	7.13 $\mu\text{V}/^{\circ}\text{C}$	0.02	$\infty$
$\delta t_{HF}$		0.005 $^{\circ}\text{C}$	Rectangular	7.13 $\mu\text{V}/^{\circ}\text{C}$	0.02	$\infty$
$\delta E_{VC}$		0.01 $\mu\text{V}$	Normal (k =1)	1	0.01	$\infty$
$\delta E_{VR}$		0.005 $\mu\text{V}$	Rectangular	1	0.003	$\infty$
$\delta E_{VD}$		0.01 $\mu\text{V}$	Rectangular	1	0.006	$\infty$
$\delta E_{SC}$		-	-	-	-	-
$\delta t_0$		0.01 $^{\circ}\text{C}$	Rectangular	6.03 $\mu\text{V}/^{\circ}\text{C}$	0.04	$\infty$
$\delta E_{IH}$		0.006 %	Rectangular	1	0.002	$\infty$
$\delta E_{EN}$		0.01 $\mu\text{V}$	Rectangular	1	0.006	$\infty$
$E_x$	196.06				<b>0.06</b>	$\gg 500$

Table A-12. Uncertainty analysis at Ag point of NMISA

Quantity $X_i$	Estimate $x_i$	Standard uncertainty $u(x_i)$	Probability distribution	Sensitivity coefficient $c_i$	Uncertainty contribution $u_i(y)$	Degree of freedom
$E_F$	16118.15	0.03	Normal (k=1)	1	0.03	2
$\delta t_F$		0.017	Rectangular	24.95	0.24	500
$\delta t_{HF}$		0.005	Rectangular	24.95	0.07	500
$\delta E_{VC}$		0.55	Normal (k=2)	1	0.28	500
$\delta E_{VR}$		0.005	Rectangular	1	0.005	500
$\delta E_{VD}$		1.65	Rectangular	1	0.95	500
$\delta E_{SC}$		0.20	Rectangular	1	0.12	500

$\delta t_0$		0.01	Rectangular	6.03	0.03	500
$\delta E_{IH}$		$1.04 \cdot 10^{-4}$	Rectangular	15976.3	0.96	3.3
$\delta E_{EN}$		0.005	Normal (k=1)	1	0.005	76
$E_x$	16118.15				<b>1.41</b>	15.3

Table A-14. Uncertainty analysis at A1 point of NMISA

Quantity $X_i$	Estimate $x_i$	Standard uncertainty $u(x_i)$	Probability distribution	Sensitivity coefficient $c_i$	Uncertainty contribution $u_i(y)$	Degree of freedom
$E_F$	9318.89	0.02	Normal (k=1)	1	0.02	2
$\delta t_F$		0.002	Rectangular	20.14	0.02	500
$\delta t_{HF}$		0.002	Rectangular	20.14	0.02	500
$\delta E_{VC}$		0.32	Normal (k=2)	1	0.16	500
$\delta E_{VR}$		0.005	Rectangular	1	0.005	500
$\delta E_{VD}$		1.11	Rectangular	1	0.64	500
$\delta E_{SC}$		0.20	Rectangular	1	0.12	500
$\delta t_0$		0.01	Rectangular	6.03	0.03	500
$\delta E_{IH}$		$1.04 \cdot 10^{-4}$	Rectangular	9177.0	0.55	3.3
$\delta E_{EN}$		0.002	Normal (k=1)	1	0.002	24
$E_x$	9318.89				<b>0.87</b>	20.1

Table A-15. Uncertainty analysis at Zn point of NMISA

Quantity $X_i$	Estimate $x_i$	Standard uncertainty $u(x_i)$	Probability distribution	Sensitivity coefficient $c_i$	Uncertainty contribution $u_i(y)$	Degree of freedom
$E_F$	4944.61	0.01	Normal (k=1)	1	0.01	2
$\delta t_F$		0.000 5	Rectangular	16.16	0.004	500
$\delta t_{HF}$		0.000 3	Rectangular	16.16	0.003	500
$\delta E_{VC}$		0.17	Normal (k=2)	1	0.08	500
$\delta E_{VR}$		0.005	Rectangular	1	0.005	500
$\delta E_{VD}$		0.76	Rectangular	1	0.44	500
$\delta E_{SC}$		0.20	Rectangular	1	0.12	500
$\delta t_0$		0.01	Rectangular	6.03	0.03	500
$\delta E_{IH}$		$1.04 \cdot 10^{-4}$	Rectangular	4802.8	0.29	3.3
$\delta E_{EN}$		0.002	Normal (k=1)	1	0.002	37
$E_x$	4944.61				<b>0.55</b>	40.3

Table A-16. Uncertainty analysis at Sn point of NMISA

Quantity $X_i$	Estimate $x_i$	Standard uncertainty $u(x_i)$	Probability distribution	Sensitivity coefficient $c_i$	Uncertainty contribution $u_i(y)$	Degree of freedom
$E_F$	2235.61	0.01	Normal (k=1)	1	0.01	2
$\delta t_F$		0.000 4	Rectangular	12.60	0.003	500
$\delta t_{HF}$		0.000 4	Rectangular	12.60	0.003	500

$\delta E_{VC}$		0.08	Normal (k=2)	1	0.04	500
$\delta E_{VR}$		0.005	Rectangular	1	0.005	500
$\delta E_{VD}$		0.54	Rectangular	1	0.31	500
$\delta E_{SC}$		0.20	Rectangular	1	0.12	500
$\delta t_0$		0.01	Rectangular	6.03	0.03	500
$\delta E_{IH}$		$1.04 \cdot 10^{-4}$	Rectangular	2093.8	0.13	3.3
$\delta E_{EN}$		0.002	Normal (k=1)	1	0.002	62
$E_x$	2235.61				<b>0.36</b>	175.1

Table A-16. Uncertainty analysis at Ga point of NMISA

Quantity $X_i$	Estimate $x_i$	Standard uncertainty $u(x_i)$	Probability distribution	Sensitivity coefficient $c_i$	Uncertainty contribution $u_i(y)$	Degree of freedom
$E_F$	196.19	0.007	Normal (k=1)	1	0.007	2
$\delta t_F$		0.000 1	Rectangular	7.13	0.000 4	500
$\delta t_{HF}$		0.000 1	Rectangular	7.13	0.000 4	500
$\delta E_{VC}$		0.007	Normal (k=2)	1	0.003	500
$\delta E_{VR}$		0.005	Rectangular	1	0.005	500
$\delta E_{VD}$		0.38	Rectangular	1	0.22	500
$\delta E_{SC}$		0.20	Rectangular	1	0.12	500
$\delta t_0$		0.01	Rectangular	6.03	0.03	500

$\delta E_{IH}$		$1.04 \cdot 10^{-4}$	Rectangular	54.3	0.003	3.3
$\delta E_{EN}$		0.001	Normal (k=1)	1	0.001	18
$E_x$	196.19				<b>0.25</b>	794

Table A-17. Uncertainty analysis at Ag point of NMIA

Quantity $X_i$	Estimate $x_i$	Standard uncertainty $U_i(\mathbf{u}(x_i))$	Sensitivity coefficient $c_i$	Probability distribution $k_i$	Uncertainty contribution $u_i(\mathbf{y}) / \mu\text{V}$	Degree of Freedom
$E_F$	16117.75	0.05	1	1	0.050	4
$\delta t_F$		0.012	24.95	2	0.150	20
$\delta t_{HF}$		0.005	24.95	2	0.062	8
$\delta E_{VC}$		0.034	1	2	0.017	50
$\delta E_{VD}$		0.355	1	2	0.177	50
$\delta E_{VR}$		0.01	1	1.73	0.006	50
$\delta E_{SC}$		-	-	-	-	-
$\delta t_0$		0.01	6.03	2	0.030	8
$\delta E_{IH}$		0.856	1	2	0.429	20
$\delta E_{EN}$		0.1	1	2	0.050	20
$E_x$	16117.35	U = 1.010 $\mu\text{V}$ ( $k = 2.03$ , $v_{\text{eff}} = 35.37$ )			<b>0.497</b>	35.37

Table A-18. Uncertainty analysis at Al-point of NMIA

Quantity $X_i$	Estimate $x_i$	Standard uncertainty $U_i(\mathbf{u}(x_i))$	Sensitivity coefficient $c_i$	Probability distribution $k_i$	Uncertainty contribution $u_i(\mathbf{y}) / \mu\text{V}$	Degree of Freedom
$E_F$	9812.62	0.02	1	1	0.02	4
$\delta t_F$		0.0013	20.14	2	0.013	20
$\delta t_{HF}$		0.004	20.14	2	0.040	8

$\delta E_{VC}$		0.034	1	2	0.017	50
$\delta E_{VD}$		0.205	1	2	0.103	20
$\delta E_{VR}$		0.01	1	1.73	0.006	20
$\delta E_{SC}$						
$\delta t_0$		0.01	6.03	2	0.030	20
$\delta E_{IH}$		0.448	1	2	0.224	20
$\delta E_{EN}$		0.1	1	2	0.050	20
$E_x$	9812.62	(k = 2.032, v <sub>eff</sub> = 34.42)			<b>0.258</b>	34.42

Table A-19. Uncertainty analysis at Zn-point of NMIA

Quantity $X_i$	Estimate $x_i$	Standard uncertainty $U_i(\mathbf{u}(x_i))$	Sensitivity coefficient $c_i$	Probability distribution $k_i$	Uncertainty contribution $u_i(\mathbf{y}) / \mu\text{V}$	Degree of Freedom
$E_F$	4944.39	0.03	1	1	0.03	4
$\delta t_F$		0.001	16.16	2	0.008	20
$\delta t_{HF}$		0.003	16.16	2	0.024	8
$\delta E_{VC}$		0.034	1	2	0.017	50
$\delta E_{VD}$		0.109	1	2	0.054	50
$\delta E_{VR}$		0.05	1	1.73	0.029	50
$\delta E_{SC}$						
$\delta t_0$		0.01	6.03	2	0.030	20
$\delta E_{IH}$		0.186	1	2	0.093	20
$\delta E_{EN}$		0.1	1	2	0.050	20
$E_x$	4944.39	U = 0.2652 $\mu\text{V}$ ( $k = 1.995$ , $v_{\text{eff}} = 69.15$ )			<b>0.133</b>	69.15

Table A-20. Uncertainty analysis at Sn-point of NMIA

Quantity $X_i$	Estimate $x_i$	Standard uncertainty $U_i(\mathbf{u}(x_i))$	Sensitivity coefficient $c_i$	Probability distribution $k_i$	Uncertainty contribution $u_i(\mathbf{y}) / \mu\text{V}$	Degree of Freedom
$E_F$	2235.5	0.03	1	1	0.030	4
$\delta t_F$		0.001	12.59	2	0.006	20
$\delta t_{HF}$		0.003	12.59	2	0.019	8

$\delta E_{VC}$		0.034	1	2	0.017	50
$\delta E_{VD}$		0.049	1	2	0.025	20
$\delta E_{VR}$		0.05	1	1.73	0.029	50
$\delta E_{SC}$						
$\delta t_0$		0.01	6.03	2	0.030	20
$\delta E_{IH}$		0.023	1	2	0.012	20
$\delta E_{EN}$		0.1	1	2	0.050	20
$E_x$	2235.5	U = 0.162 $\mu$ V ( $k = 1.994$ , $v_{eff} = 71.17$ )			<b>0.081</b>	71.17

Table A-21. Uncertainty analysis at Ga-point of NMIA

Quantity $X_i$	Estimate $x_i$	Standard uncertainty $U_i(\mathbf{u}(x_i))$	Sensitivity coefficient $c_i$	Probability distribution $k_i$	Uncertainty contribution $u_i(\mathbf{y}) / \mu\text{V}$	Degree of Freedom
$E_F$	196.11	0.01	1	1	0.01	4
$\delta t_F$		0.0005	7.12	2	0.002	20
$\delta t_{HF}$		0.002	7.12	2	0.007	8
$\delta E_{VC}$		0.034	1	2	0.017	60
$\delta E_{VD}$		0.004	1	2	0.002	20
$\delta E_{VR}$		0.05	1	1.73	0.029	50
$\delta E_{SC}$						
$\delta t_0$		0.01	6.03	2	0.030	20
$\delta E_{IH}$		0.012	1	2	0.006	20
$\delta E_{EN}$		0.05	1	2	0.025	20
$E_x$	196.11	U = 0.106 $\mu\text{V}$ ( $k = 1.985$ , $v_{\text{eff}} = 96.05$ )			<b>0.053</b>	96.05